PB-223 960

# MECHANISMS OF FORMATION AND COMPOSITION OF PHOTOCHEMICAL AEROSOLS.

M. Lipeles, et al

Rockwell International Corporation
Thousand Oaks, California

September 1973

DISTRIBUTED BY:

NTIS

National Technical Information Service
U. S. DEPARTMENT OF COMMERCE
5285 Port Royal Road, Springfield Va. 22151

PB 223 960





SC537.10FR

# MECHANISMS OF FORMATION AND COMPOSITION OF PHOTOCHEMICAL AEROSOLS

## Final Report

(Contract 68-02-0562-CAPA-8-71)

Submitted to

Environmental Protection Agency
Durham, North Carolina 27701

and

Coordinating Research Council
New York, New York 10020

Reproduced by
NATIONAL TECHNICAL
INFORMATION SERVICE
U S Department of Commerce
Springfield VA 22151

Science Center
Rockwell International

| BIBLIOGRAPHIC DATA SHEET | 1. Report No. CRC-APRAC-CAPA-8-71-1 | 2. | 3. Recipient's Accession No. PB-223 960 |
|---|---|---|---|
| 4. Title and Subtitle: Mechanisms of Formation and Composition of Photochemical Aerosols | | | 5. Report Date: September 1973<br>6. |
| 7. Author(s): M. Lipeles, C.S. Burton, H.H. Wang, E.P. Parry G.M. Hidy | | | 8. Performing Organization Rept. No. SC537.10FR |
| 9. Performing Organization Name and Address: Rockwell International, Science Center, P O. Box 1085, 1049 Camino Dos Rios, Thousand Oaks, California 91360 | | | 10. Project/Task/Work Unit No. CRC-APRAC-CAPA-8-71<br>11. Contract/Grant No. |
| 12. Sponsoring Organization Name and Address: Coordinating Research Council, Inc. 30 Rockefeller Plaza, New York, N.Y. 10020 and Environmental Protection Agency, Durham, North Carolina 27701 | | | 13. Type of Report & Period Covered: Final<br>14. |

15. Supplementary Notes

Releasable to the public October 1973

16. Abstracts

The report details a feasibility study of a flow reactor concept for the study of the mechanism of formation and composition of photochemical aerosols. The technique involves a fast flow reactor which may be operated in a "wall free" mode. Aerosols have been produced in this reactor from a light irradiated gas mixture including $NO_2$, 1-hexene, $SO_2$, $H_2O$, and air. The chemical composition of these aerosols has been analyzed. Aerosols were also sought in a $NO_2$, 1-hexene, and dry air mixture but have not yet been obtained.

The report includes preliminary design studies and experimental study carried out under a joint contract with Environmental Protection Agency (EPA and Coordinating Research Council (CRC) and, ~~for completeness,~~ a discussion of related aspects of a ~~Science Center~~ funded study of ~~aero~~ aerosol formation in ozone-olefin reactions.

17. Key Words and Document Analysis. 17a. Descriptors

Ozone
Olefins
Flow Reactor
Irradiation
Inorgaic Gas
Organic Gas
Aerosol
Sulfate
Nitrate

17b. Identifiers/Open-Ended Terms

17c. COSATI Field/Group 15B; 7B; 7C;111.

| 18. Availability Statement | 19. Security Class (This Report) | 21. No. of Pages |
|---|---|---|
| Releasable to the general public. | UNCLASSIFIED | 100 104 |
| | 20. Security Class (This Page) UNCLASSIFIED | 22. Price $4.25 |

FORM NTIS-35 (REV. 3-72) 14. THIS FORM MAY BE REPRODUCED USCOMM-DC 14952-P72

# MECHANISMS OF FORMATION & COMPOSITION OF PHOTOCHEMICAL AEROSOLS

Final Report

(Contract 68-02-0562-CAPA-8-71)

Submitted to

Environmental Protection Agency
Durham, North Carolina 27701

and

Coordinating Research Council
New York, New York 10020

Prepared by

M. Lipeles
with
C. S. Burton
H. H. Wang
E. P. Parry
and
G. M. Hidy

Science Center
Rockwell International

TABLE OF CONTENTS

| | Page |
|---|---|
| Abstract | i |
| 1. Introduction | 1 |
| 1.1 Goals and Method | 2 |
| 1.2 Accomplishments | 2 |
| 2. Observations and Simulations of Photochemical Aerosols | 4 |
| 2.1 Field Observations | 4 |
| 2.2 Laboratory Studies | 11 |
| 2.3 Goals of Aerosol Simulation | 14 |
| 2.4 Approach of the Flow Reactor Experiment | 16 |
| 3. The Flow Reactor System | 19 |
| 3.1 Reactor Design Principles | 19 |
| 3.2 Detailed Description of Experimental System | 30 |
| 3.2.1 The Reactor Section | 33 |
| 3.2.2 Gas Handling | 33 |
| 3.2.3 Irradiation | 34 |
| 3.2.4 Sampling | 36 |
| 3.2.5 Measurement Techniques | 43 |
| 4. Experimental Results and Discussions | 45 |
| 4.1 Gas Phase Chemistry | 45 |
| 4.1.1 Inorganic Gas Phase Tests | 45 |
| 4.1.2 Organic Gas Phase Tests/GC Measurements | 47 |
| 4.2 Aerosols Experiments | 51 |
| 4.2.1 Ozone-Olefin Aerosols | 52 |
| 4.2.2 Flow Reactor Aerosol Experiments | 52 |
| 4.3 Chemical Analysis of the Aerosol Samples | 55 |
| 4.3.1 Sulfate Analysis | 55 |
| 4.3.2 Nitrate Analysis | 59 |
| 4.3.3 Total Organic Analysis | 60 |
| 4.4 Discussion of Aerosol Results | 61 |
| 5. Summary and Recommendations | 64 |
| 5.1 Aerosol Production | 64 |

| | Page |
|---|---|
| 5.2 Chemical Analysis | 64 |
| 5.3 Data Analysis and Feasibility | 65 |
| 5.4 Recommendations | 65 |
| Appendix A. Modeling, Mechanism and Simulation | 66 |
| A.1 Scaling of Reactions | 66 |
| A.2 Extrapolation of Laboratory Experiments to Atmospheric Transformations | 71 |
| A.3 Mathematical Modeling of Gas Phase Kinetics | 74 |
| Appendix B. Aerosol Forming Reactions with Ozone & Olefins in a Flow Reactor | 81 |
| B.1 Experimental Methods | 81 |
| B.2 Experimental Results & Discussions | 83 |
| B.3 Chemical Analysis of Ozone-Olefin Aerosol | 91 |
| References | 95 |

ABSTRACT

This report details a feasibility study of a flow reactor concept for the study of the mechanism of formation and composition of photochemical aerosols. The technique involves a fast flow reactor which may be operated in a "wall free" mode. Aerosols have been produced in this reactor from a light irradiated gas mixture including $NO_2$, 1-hexene, $SO_2$, $H_2O$, and air. The chemical composition of these aerosols has been analyzed. Aerosols were also sought in a $NO_2$, 1-hexene, and dry air mixture but have not yet been obtained.

The report includes preliminary design studies and experimental study carried out under a joint contract with Environmental Protection Agency (EPA) and Coordinating Research Council (CRC)* and, for completeness, a discussion of related aspects of a Science Center funded study of aerosol formation in ozone-olefin reactions.

*This is under the Air Pollution Research Advisory Committee (APRAC) of CRC. APRAC represents API, MVMA, and EPA.

## 1. Introduction

One of the major problems confronting modern civilization is the continuing degradation of air quality in major urban complexes. An important symptom of air pollution is the increased concentration of airborne particulates over cities, resulting in increased health hazards, decreased visibility, and corrosive destruction of property. The formation of aerosols by man's activity is perhaps the most easily identified manifestation of air pollution. However, the details of the mechanisms of formation of airborne particles and their evolution and removal from the atmosphere, remain poorly understood despite considerable effort devoted to this subject.

A number of years ago, workers recognized that aerosol particles could appear in the atmosphere via two different routes. The first involves primary emissions from sources such automobile exhaust, or smokestacks. The other is secondary in nature, where particles are produced by physicochemical processes in the atmosphere itself. The possibility of chemical aerosol formation was probably first demonstrated by Tyndall in the 19th century.[1] The significance of such a mechanism for removal of reactive trace gases from the atmosphere has not been fully appreciated until recently.[2]

There is mounting evidence that the formation of aerosols by photochemical reactions in the atmosphere plays a significant local role in air pollution over many cities. In fact, the formation of a haze of such suspended material is an integral part of photochemical smog. It was recognized in the classical work on smog reactions[3] that aerosols would form in photochemically reactive atmospheres containing hydrocarbon vapors, water vapor, and nitrogen oxides. More recent studies in smog chambers have elucidated the relation between $SO_2$ and photochemical aerosol formation.[4-7] Other work, such as that of Bricard *et al.*[8] and Goetz and coworkers[9], have indicated that significant gas-particle interactions take place in air containing pollutant gases irradiated by sunlight.

## 1.1 Goals and Method

In response to APRAC request for proposals for experimental work on the mechanism of formation and compositon of photochemical aerosols, we proposed a novel method to produce and study aerosols in a fast flow reactor. This report covers a feasibility study performed under APRAC contract. The objectives of this study are to (a) determine if light scattering airborne particles can be produced in an air flow containing hydrocarbon vapors and nitrogen oxides, (b) analyze such particles for their chemical composition, and (c) determine the feasibility of using a flow reactor for simulation of photochemical generation of aerosols in polluted atmospheres.

The flow reactor employed maintains laminar flow in an irradiated section with a residence time of a few seconds to a minute. The gases and aerosols are sampled by a variety of probes and filters and analyzed by many methods. In the case of the organic component of the aerosol we are able to employ infrared spectroscopy and gas chromatography (GC) with a mass spectrometer detector (GC-MS). For the inorganic components of the aerosol techniques include spectrophotometry, pulse polarography, and standard wet chemical methods. For gas phase analysis we employ standard chemiluminescent instruments and GC. For physical analysis of aerosols we have used condensation nuclei counters and optical particle counters and have available several methods of total mass monitoring.

## 1.2 Accomplishments

In this program we have designed, constructed, and tested a flow reactor for the production of aerosols in controlled experiments. The testing carried out under the APRAC contract was in the nature of a feasibility study. The main goal was the generation of aerosols in the reactor in an irradiated mixture of $NO_x$, air, hydrocarbons, and possible additional trace components. We have observed aerosols in one such system: $NO_2$, air, 1-Hexene, $SO_2$, and $H_2O$.

Attempts to produce aerosols with only $NO_2$, dry air, and an olefin, irradiated in the flow reactor, with residence times of a few seconds, have not to date produced aerosols. Due to limitations of time, we did not

completely characterize the products or obtain completely consistent gas phase data during the unsuccessful aerosol production tests.

In general during the testing of the reactor, qualitative agreement with expected results was accepted due to time considerations. By qualitative agreement, we mean that if an expected product was found within a factor of 10 of the expected concentration, this was satisfactory. If effects such as the peaking of a product concentration with the variation of a parameter appeared roughly as expected, this was satisfactory. Unfortunately in some cases, particularly the estimation of the light intensity, this led to large uncertainties in the analysis of the data.

The aerosols produced in the $SO_2$, 1-hexene, $NO_2$ system were collected and analyzed for composition. These analyses included (a) $SO_4^=$, which was definitely present, (b) $NO_3^-$ which was detected but may have a contamination problem in the collection method, and (c) total organics which were less than a few micrograms in a 100 μgm sample. Techniques for chemical analysis were also tested on organic aerosols produced in another reactor from pure ozone-olefin reactions in dry air. Because this work bears on the flow reactor experiment, these simpler experiments are described in Appendix B, although these experiments with ozone and olefins were funded separately by the Science Center.

We therefore conclude that we have demonstrated the feasibility of producing aerosols in a fast flow reactor. It should now be possible to attempt to completely analyze the $NO_x$, air, olefin system to find the conditions, in this reactor or a similar one, for which aerosols are produced, and to determine the applicability of such data to aerosol formation in urban atmospheres. This will be supported by our improved kinetic modeling capabilities which are discussed in Appendix A.

## 2. Observations and Simulations of Photochemical Aerosols

In the first two parts of this section we will review field observations and experimental simulations of photochemical aerosols. Following that we will draw these two together into a set of goals for aerosol simulation and then discuss our approach to this problem.

### 2.1 Field Observations

Knowledge of photochemical aerosol formation in urban atmospheres remains incomplete. However, there are considerable data accumulated by the National Air Surveillance Network (NASN)[10] suggesting that aerosols in a photochemically active atmosphere differ significantly from aerosols sampled in air where photochemical reactions are less important. For example, the former case reveals an enrichment in nitrates and benzene soluble hydrocarbons.

A recent survey of information on the Pasadena aerosol suggested that more than one-third of the airborne material sampled was of secondary origins.[11] Despite the fact that the total aerosol mass observed is only a small fraction of the total trace material loading of the atmosphere, the suspended particles are particularly significant in their ability to act as carriers of toxic matter to the lower respiratory system and as the major factor in visibility degradation.

Investigations of aerosols in the atmosphere have revealed a highly complicated behavior that is far from being characterized in any detail. There is comparatively little information available about the mechanism of formation and evolution of airborne particles, making the specification and development of a quantitative simulation model difficult. Suspended particles have been shown to have highly complicated chemical composition that originates from a variety of natural and anthropogenic sources. The mixture of material is from primary and secondary sources. Some elements such as silicon and lead are identified with primary emissions such as auto exhaust and dust rise by wind. Other compounds are related extensively to secondary processes, including $SO_4^{=}$, $NO_3^{-}$, $NH_4^{+}$, and possible hydrocarbons. Studies in photochemically reactive and non-reactive urban atmospheres have shown both differences and similarities in aerosol properties, some of which are listed in Table 1. In

## Table 1

Speculated Differences and Similarities in Physical Properties Between Photochemically Active and Non-Active Urban Atmospheres

1. While the average number of aerosol particles is greater for a photochemically active atmosphere, the peak number, as reflected by Aitken nuclei concentration is much larger for non-photochemically active atmosphere. (Data from Ref. 60)

| | $N_T$ (Ground Average) | Daily Peak |
|---|---|---|
| Los Angeles | $1.14\times10^5$ $cm^{-3}$ | $\sim 2\times10^5$ $cm^{-3}$ |
| Minneapolis | $(2.1 \text{ to } 6.6)\times10^4$ $cm^{-3}$ | $\sim 2\times10^6$ $cm^{-3}$ |

2. The volume arithmetic mean radii of aerosol particles in a photochemically reactive atmosphere are smaller than in a non-active atmosphere (Data from Ref. 60).

   Dpvm (Los Angeles) - 0.086 μm

   Dpvm (Minneapolis) = 0.09 to 0.11 μm

3. Light scattering and visibility reduction in photochemically reactive atmospheres may follow the change in ozone concentration (See Fig. 1).

4. The particle size spectra measured in both show broad features that may be correlated in terms of self-preserving "similarity variables." However, both exhibit strong diurnal fluctuations in particle concentration in submicron size ranges and below (60).

5. Both photochemically active and non-active urban atmospheres show a bi-modal distribution of mass with particle size. The pollutant aerosols appear to be mainly in the range of submicron size while natural particles appear to be more strongly correlated with larger particles (60).

photochemically active atmospheres, such as that of Los Angeles (LA), there is a larger average number concentration, but a much smaller daily peak number of Aitken nuclei, and a smaller mean particle radius compared with a non-photochemically dominated atmosphere like Minneapolis. Furthermore, the LA atmosphere is enriched in nitrates and benzene soluble hydrocarbons. The average composition of a typical sample of the Los Angeles aerosol is shown in Table 2. From these data, it can be seen that simulation in the laboratory of the aerosol samples in a "real," typical photochemical reactive atmosphere would be very difficult and probably impractical.

The constituents that have been identified as dominated by atmospheric transformations include oxidized nitrate, sulfur, and carbon compounds. Perhaps most extensively studied of these three are the sulfate forming reactions through oxidation of $SO_2$, either by homogeneous gas phase reactions or by heterogeneous transformations in the presence of liquid water and cations such as $NH_4^+$ or metal ions. The possible reactions of hydrocarbon aerosols in the atmosphere which lead to nitrate formation are poorly defined at this time. Indeed, there remain serious questions about the nature of nitrate in aerosols, particularly if nitrous or nitric acid are involved. The high volatility of nitric acid compared with sulfuric acid, for example, points to a potentially significant distinction between homogeneous nucleation of such material vs. heterogeneous processes. The mechanisms for formation of organic aerosols in the atmosphere remain a mystery. Presumably condensed material of a polymeric form, or a highly oxygenated form can be derived from reactions involving unsaturated materials of carbon number higher than three to four. However, these must be in competition with other mechanisms that would reduce the molecular weight of reactive intermediates such as ozonides or hydroperoxides as a result of decomposition reactions in the presence of water vapor. Based on current knowledge, it would appear that only 0.1% to 1% of the reactive hydrocarbons in the polluted atmosphere are converted to condensed material on the time scale of several hours.

There is mounting evidence that water is intimately involved in different ways in aerosol formation. Charlson and colleagues, for example, have shown

Table 2

Chemical Component List for the Pasadena Aerosol from Averages of Data Sampled in Smog During Late Summer 1969

(after Miller et al., Ref. 12)

| Component | Concentration (Wt. %) |
|---|---|
| Na | 1.7 |
| K | 0.56 |
| Mg | 0.69 |
| Ca | 1.2 |
| Ba | $2.9\times10^{-2}$ |
| Ti | 0.5 |
| V | $9.5\times10^{-3}$ |
| Mn | $2.6\times10^{-2}$ |
| Fe | 3.4 |
| Cu | $4.3\times10^{-2}$ |
| Zn | 0.25 |
| Aℓ | 0.33 |
| C (non-carbonate) | 28 |
| Si | 0.74 |
| Pb | 4.6 |
| Cℓ | 0.03-0.6 |
| Br | 1.2 |
| I | $4.8\times10^{-3}$ |
| $NH_4^+$ | 0.8 |
| $NO_3^-$ | 1.8 |
| $SO_4^=$ | 12 |
| Unidentified | 42.2 |
| Total | 100.0% |

that the light scattering urban aerosol increases with relative humidity (R.H.), particularly above 50% R.H.[13] Recent work of W. Ho[14] during the 1972 aerosol observational program in Los Angeles indicates that the liquid water content of atmospheric aerosol may display a diurnal variation closely linked with changes in aerosol mass, $b_{scat}$, and photochemical reactants such as $NO_x$ or $O_3$. Unquestionably water is potentially involved in $SO_4^=$, $NO_3^-$, and oxygenated hydrocarbon stabilization in aerosols. Thus, the role of this most universal and prevalent of all atmospheric "trace" gases must be accounted for in aerosol formation mechanisms.

To add to the difficulties in interpretation of aerosol simulation, the kinetics of aerosol behavior have to be included. There is little information on the daily evolution of aerosols in photochemical smog. Perhaps the most detailed field investigation of photochemical aerosols, completed to date in the Los Angeles atmosphere,was conducted in a comparative study in 1969.[15] This study attempted to measure, in as detailed a way as possible, the physical and chemical properties of photochemical aerosols as a function of time under conditions ranging from light to moderately heavy smog in Pasadena, California. Results of this field program revealed that there was a strong correlation between the behavior of aerosols and the daily evolution of trace gas concentrations associated with smog.

Results for the average diurnal variation in gas concentration and aerosol properties for Pasadena in 1969 are shown in Figs. 1 and 2. The pattern of behavior of the trace gases is typical of that known for photochemical smog in Los Angeles. The striking feature of the aerosol data is that the smallest particles, represented by the total number density of Aitken nuclei concentration, $\langle N \rangle$, follows a pattern quite different from the larger particle fractions, characteristic of the average surface area for unit volume, $\langle S \rangle$, and the volume fraction, $\langle \phi \rangle$. The larger particle fractions display a mid-day peak with ozone while the Aitken nuclei peak late in the afternoon. This may imply that much of the photochemical interaction with particles is manifested in the larger particles. Husar, Whitby, and Liu[16] have attempted to interpret these physical dynamics in terms of formation and growth mechanisms. Their interpretations suggest that aerosol growth during

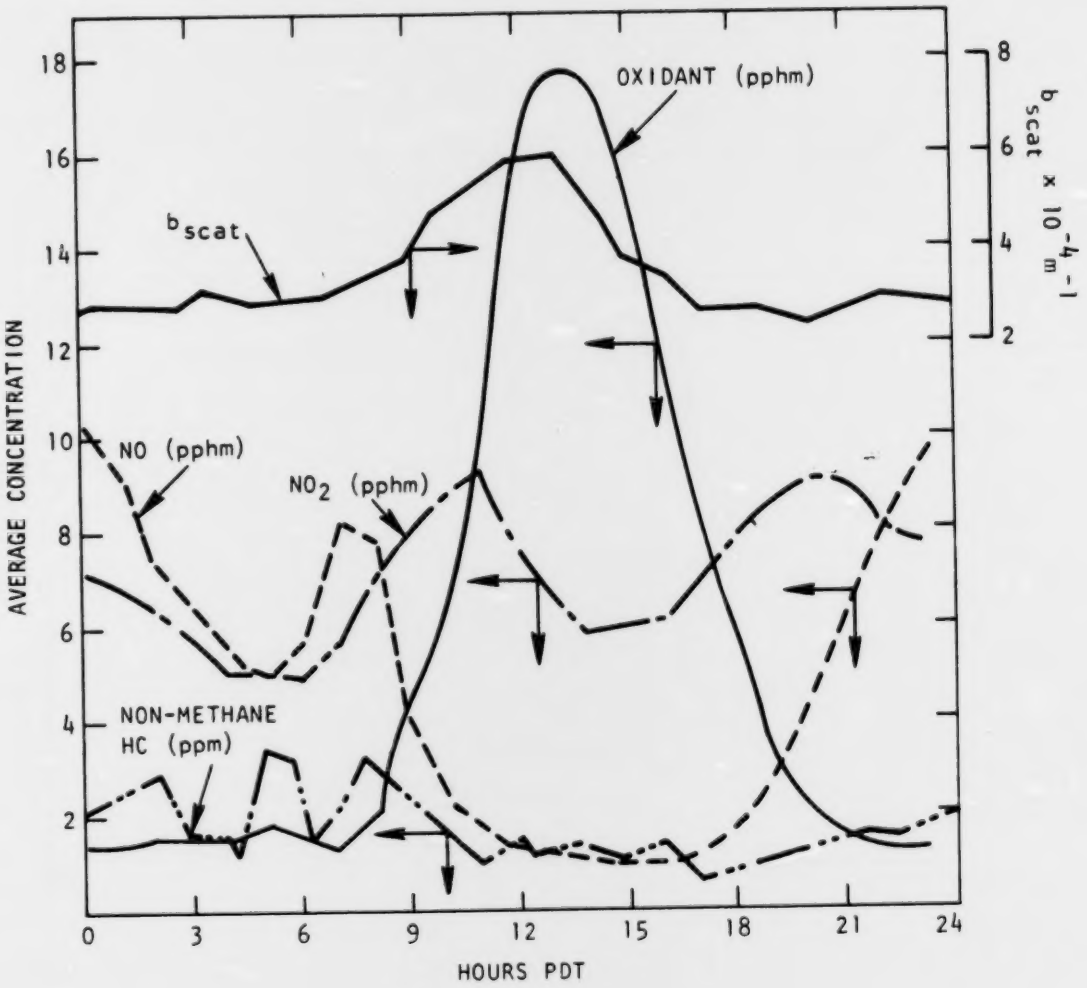


Fig. 1 Diurnal variation in trace gases and in light scattering by nephelometry, in photochemical smog based on composited data from the 1969 Pasadena study.[17]

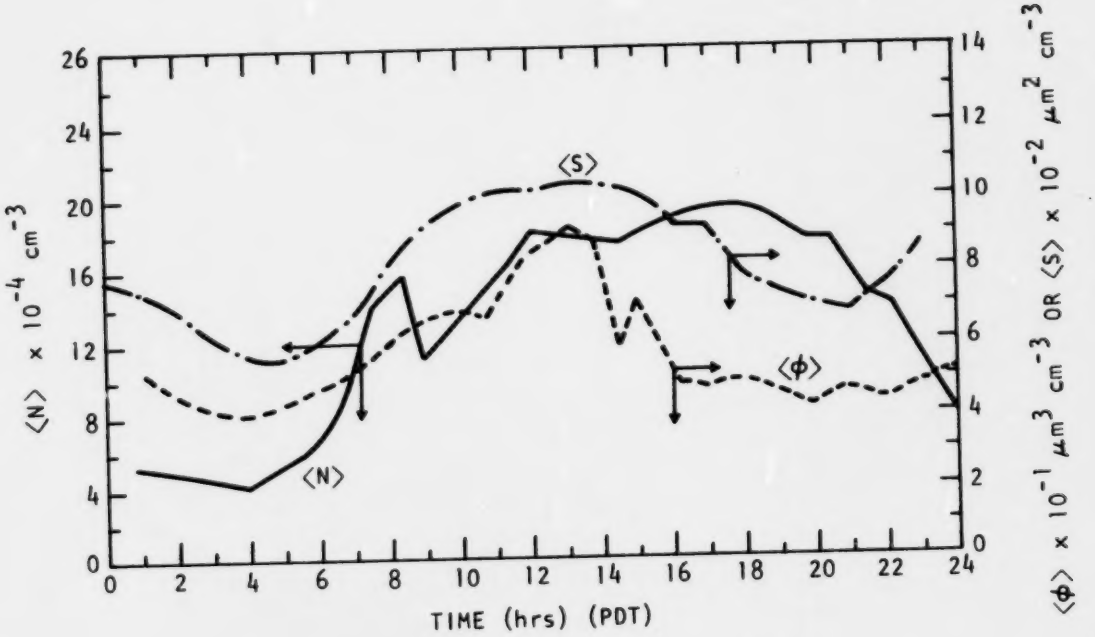


Fig. 2 Average diurnal behavior of photochemical smog aerosol properties based on the 1969 Pasadena study.(17) <N> represents the mean Aitken nuclei concentration, <S> the average surface area per unit volume, and <$\phi$> the volume fraction.

the daylight hours is dominated by condensation on 0.1-1 μm size particles and that this condensation is dependent upon the photochemical activity in the atmosphere. New nuclei primarily enter into the atmosphere directly from combustion sources except in the early morning when the concentration of 0.1-1 μm particles is small and homogeneous nucleation may take place. Coagulation was shown to have negligible effect except late at night (after 2300 hrs) when both sources and photochemistry are at a low level. It was also suggested by Hidy et al.[17] that the condensation process may include reactions directly on the particles of photochemically produced materials.

## 2.2 Laboratory Studies

For almost two decades the chemistry of polluted atmospheres has been simulated and measured in laboratory studies. Extensive information has been obtained about the gas phase reactions so that we have a knowledge of their salient features.[18-19] This work continues and new observations and clarifications are still being made. For example, although previously neglected as a reactant, an effect of CO has been observed[20] and a dramatically improved nitrogen material balance has been achieved with the identification of $HNO_3$ on the chamber walls.[21]

The level of knowledge of the gas phase part of photochemical smog is such that new, highly speculative mechanisms are still being proposed from time to time. Nevertheless, the role of $NO_2$ molecules as photoabsorbers, the resultant oxygen atoms as initiators, and some sort of free radical chains are accepted concepts. Complex kinetic models, which incorporate these ideas, are now being introduced to attempt to describe the overall reactions and serve as input to dynamical atmospheric models.[22-24] These models give at least qualitative agreement with atmospheric and smog chamber results, although important discrepancies still exist.

The formation of aerosols is much less well understood or even studied from a laboratory point of view. Although Haagen-Smit demonstrated the formation of aerosols in the laboratory in his pioneering work on photochemical smog,[25] progress in laboratory simulation of aerosols has been slow. Aerosols are much more difficult to control, simulate, and measure than

gases and appear to be more dependent on trace constituents which may not necessarily play a significant role in the gas phase reactions. Nevertheless, several groups have been active and there is a body of knowledge on the simulation of aerosols.

After Haagen-Smit's work, a group at the Stanford Research Institute did a series of studies on aerosol formation.[26] They first demonstrated that automobile exhaust, when irradiated, produced aerosol particles in the 0.25 to 1 μm size range. The condensation nuclei were measured and showed initially high concentration with a lower steady state concentration. They went on to measure the chemical composition of these particles and found nitrate, sulfate, and both water soluble and ether soluble organics. These accounted for about 85% by weight of the material. They then tried various mixtures of individual hydrocarbons with $SO_2$ and NO. In conjunction with these experiments, a group at the Franklin Institute carried out a similar series of experiments.[27] Generally, these observers found in the absence of $SO_2$ many nitric oxide-hydrocarbon systems produced some aerosol. The largest amounts were associated with branched-chain internal olefins, cyclo-olefins, and diolefins. The introduction of $SO_2$ at the start of the reactions dramatically increased the aerosol formation and aerosols were produced even for those systems that produced none without $SO_2$. The Franklin Institute group showed that the $SO_2$ had to be present from the start to have its greatest effect. These experiments were all carried out in stirred or stirred flow type reaction vessels of various sizes.

A rather extensive series of experiments were carried out by A. Goetz and his colleagues using a non-turbulent flow reactor.[9,28] In addition to various gases, monodispersed latex aerosols were introduced into the reactor channel. They found that when an $NO_2$ and 1-octene mixture in air is irradiated, the latex aerosols grow in mass and that the total added mass is linearly related to the aerosol concentration. In the absence of external nuclei they observed the spontaneous appearance of nuclei. Then they carried out an extended study of various permutations of reactants and conditions and found that in the absence of $SO_2$ the largest amount of light scattering aerosols was produced at low humidity. However, they also found that

aerosol formation depended upon the order in which they mixed the reactants before irradiating. They corroborated the fact that $SO_2$ increases the aerosol formation, but made the interesting observation that at low $SO_2$ concentration the aerosol formation is inhibited dramatically especially for higher humidity.

Aerosol formation in a flow reactor was studied by Stevenson, Sanderson, and Altshuller.[5] Their experiments corroborated many of the observations of the Stanford research group but also included a study of the effects of mixing two hydrocarbons. The addition of trans-2-butene to cyclohexene increased aerosol production by a factor of 10 when the two hydrocarbon concentrations were equal but when the trans-2-butene concentration was increased to several times the cyclohexene concentration, the effect began to reverse. Additional observations have been made by Harkins and Nicksic[29] in which $SO_2$ produced aerosols contained no organic material.

More recent work of Wilson and Levy[4] is important in the motivation of our work. They found that in a stirred reactor the aerosol formation rate was increased by turning off the stirring. An important aspect of this observation is that the stirring is not removing aerosol once it is produced, but it inhibits the production of aerosol. This was shown by producing aerosol without stirring and looking at its subsequent behavior with stirring. In this case once formed, the aerosol lifetime is not reduced enough by stirring to account for the decrease in formation with stirring.

Two recent series of experiments by Groblicki and Nebel[6] and by Cox and Penkett[7] are very important in that they have established that $SO_2$ can be oxidized, by organic material, to form sulfate aerosols. In Groblicki and Nebel's experiments, both the dark reactions of ozone and olefins and the photolysis of $NO_x$ and olefins, oxidize $SO_2$, in presence of $H_2O$, to form aerosols. In the irradiated case the presence of NO inhibited both ozone, as is known, and aerosol formation. Cox and Penkett studied the formation of aerosols from $SO_2$ and $H_2O$ in the presence of products of ozone-olefin reactions in great detail, concluding that these products are efficient oxidizing agents for $SO_2$. They also noted that the presence of molecular oxygen was not necessary. They have extensive rate data on consumption of ozone and olefins and for-

mation of aerosol for various conditions and various aerosols. The aerosols formed in these experiments by both groups were apparently pure sulfate material. Groblicki and Nebel also produced aerosols with organic material from ozone-olefin reactions but only in the absence of $SO_2$ and only for certain olefins.

Although under certain conditions organic aerosols are produced in smog chambers, few extended efforts to analyze them have been undertaken. One noteworthy effort was made at Battelle[30] in conjunction with a field program. Gas chromatography-mass spectroscopy was used to analyze aerosols produced in the photolysis of $NO_2$ and either α-pinene, cyclohexene, or 1-heptene. In each case a few of the components were tentatively identified.

Clearly a great amount of work remains to be done in elucidating the nature and mechanisms of formation of aerosols in the atmosphere. Even under controlled laboratory conditions experiments are not understood completely and the extension of these results to the atmosphere is still tenuous.

## 2.3 Goals of Aerosol Simulation

Putting together the material in sections 2.1 and 2.2, we obtain a very complex picture of the behavior of aerosols as they interact with gases. In planning an experiment for the simulation of atmospheric aerosols, one must extract from this picture a set of goals, based on hypotheses about the nature of chemical transformations. The ultimate goal is the complete explanation of the formation and behavior of aerosol particles in polluted urban atmospheres. This must be achieved by certain subgoals, related to individual properties of aerosol particles and the gaseous chemical systems from which they form. Information must be generated which will allow a reconstruction, from individual pieces of information of the overall aerosol behavior. As a first step, we project the properties of aerosols to be simulated and the potential systems which must be studied. This is not limited to the specific work of the present contract but can cover more general experimental programs in this area.

We will now specify individual properties of aerosols in photochemical smog which must be accounted for in a simulation experiment.

1) Photochemical nucleation of new aerosol particles.

Filtered nuclei free, polluted air will on exposure to sunlight produce new nuclei.[8,16] There is some evidence that this is an important mechanism for certain short times in the atmosphere, particularly in early morning.[16]

2) Growth of 0.1 to 1 μ particles under photochemically active conditions.

This is believed to be a dominant effect, at midday, based on studies of aerosol size distributions.[16]

3) Presence of organic materials in aerosols.

A major component of photochemical aerosols is non-carbonate carbon.[12]

4) Presence of sulfate in aerosols.

Sulfate is an important component of aerosols even when the $SO_2$ concentration is low.[12]

5) Presence of nitrate and ammonium in aerosols.

Both oxidized and reduced nitrogen are found in aerosols collected in photochemical smog.[12]

6) Large increase in relative humidity causes a large increase in light scattering.[13]

7) Liquid water is present in aerosols.

Liquid water content of aerosols is positively correlated with light scattering including cases examined in photochemical smog.[14]

Many laboratories have produced data which may be related to these properties. Aerosol production and growth in many different chemical systems have been observed. The photolysis of $NO_2$, air, and many olefins both with and without water vapor has been shown to produce aerosols, as well as the photolysis of $SO_2$, water vapor, and "relatively clean" air. Combinations of these two principal mixtures also show an enhancement over each separately. What is needed, to improve on and clarify all previous experiments, is data detailed enough to specify more exactly the mechanism of aerosol production in each of these cases and any other which can be identified. This will provide a means of extrapolating to a variety of atmospheric conditions.

Thus the goal is to account for the aerosol properties outlined, as well as any new ones identified as field work progresses, by detailed care-

fully controlled study of specific individual mechanisms for aerosol formation and growth. In the next section we will discuss the Rockwell International approach to this problem under APRAC contract.

## 2.4 Approach of the Flow Reactor Experiment

In the presently reported effort we have started the development of techniques to improve the study of the formation and composition of photochemical aerosols. The most important feature of these techniques is the use of a flow reactor to eliminate the walls from affecting the reacting gases. In this way we also gain reproducibility without preconditioning the reactor. The other important feature is to employ every practicable method to achieve a total material balance for the aerosol particles and for the gas phase. We intend to carry this out for simple cases with, for example, only one hydrocarbon present.

In order for the reactor to be truly wall free, it must satisfy certain criteria. It must be true that no material produced at the walls is collected or detected as a reaction product. It is also necessary that no material, either initial or produced in the reaction, is lost to the walls of the reactor, including both products and intermediates. This last point is important in that the loss or destruction of an intermediate at the walls may change the ultimate products. This leads to the last criteria which is that no material produced at the walls react in the reactor to remove any key component of the system. These criteria are collected in a slightly different form in Table 3. In section 3.1 the constraints, brought about by these criteria, for laminar flow in a tubular reactor, are evaluated quantitatively.

An important reason for selecting a flowing reactor involves sampling of the reaction products. A very large completely static reaction chamber can conceivably meet the requirements set forth but any attempt to sample it will produce convection and turbulence and thus reintroduce the walls as an interference. In the flowing reactor the products are sampled before material has had time to diffuse to and from the walls and the sampling can be adjusted so as not to disturb the flow. The results obtained in this manner will be reproducible without any reactor pre-conditioning.

The satisfying of these criteria for a flowing system, however, requires a very short residence time compared with the expected overall reaction times. For example for the small tube (5 cm dia) used in this study, only a few seconds of residence time are allowed for meeting these criteria. The potential solution to these problems in studying the aerosol formation and growth involves two types of what we shall refer to as time scaling. These will now be defined:

a) Differential Time Scaling is the stepping to a later time in a complex reaction by setting all reactant concentrations to those which will pertain at the selected time including all intermediates and products.

b) Total Time Scaling is the adjusting of the initial conditions (concentrations, light intensity, temperature, etc.) of a complex reaction so that the overall reactions will take place at a faster rate without changing the final products, though possibly changing their relative final concentrations.

Our study employs both of these methods simultaneously and their achievement will now be discussed. The differential scaling involves no intrinsic error provided that all of the concentrations of reactants, intermediates and products can be reproduced and achieved; once it has been achieved, the reaction proceeds just as it would have if the induction period which was skipped had actually taken place. There are two problems with this method however. The rate of reaction for the remaining portion of the reaction may still be too slow for the time available. If this deviates only by a small factor, then a study of the period of time available will allow one to then proceed differentially to another point in time. If the complete reaction takes place over only a few such steps, the reaction mechanism may be studied and understood over this period. However, if this is not possible, one may further resort to total time scaling on top of the differential scaling. The other problem of differential scaling is that it may be difficult to know the exact conditions at a later time in a complex reaction. Toward this end we are helped, however, by the fact that most intermediates come into equilibrium rapidly and therefore take care of themselves, so only the principal reactants and products need be considered.

Total time scaling is more complex and does not hold in general. It should be immediately clear however that any complex set of reactions which have a rate limiting step of non-zero order in any reactant may be scaled by increasing the concentration of that reactant. If the rate limiting step depends on several reactants, then higher order scaling is possible up to the order to the rate limiting step. For example, if the rate limiting step is 3rd order and each reactant in this step is scaled by a factor of m, then the rate scales by a factor of $m^3$. Of course, the reactants in the rate limiting step are not necessarily the initial reactants, but if the rate limiting reactants depend in some simple way upon the initial reactants, then the scaling can be related to the initial reactants.

Since no complete model exists for photochemical aerosol production, it is difficult to work out possible scaling relations for aerosols. However, it is known that aerosols do not form until after the NO has been converted to $NO_2$ and there is an appreciable $O_3$ concentration. Thus in our experiments we apply the concepts of differential time scaling and total time scaling as a first approach to the problem keeping in mind the limitations of these concepts. The concept of differential time scaling is applied by starting with $NO_2$-hydrocarbon system rather than a NO-hydrocarbon system. Since $O_3$ reactions with olefins produce aerosols (See Appendix B) and O reactions with olefins in the presence of $O_2$ should have similar chemistry (see section 4.12), the concept of total time scaling is applied by increasing the $NO_2$ concentration and light intensity (thereby increasing the O atom and $O_3$ concentration) and by increasing the hydrocarbon concentration from the atmospheric concentration values.

We have also set as a goal for the experiments the characterization as completely as possible of all reaction products. This includes both gas phase and aerosol products. In this way we eventually hope to characterize conditions under which aerosols were both produced and not produced and to have a material balance for these cases. Further when aerosols are produced, we hope to obtain a material balance for the aerosol as well as a good physical characterization of it.

## 3. The Flow Reactor System

We will now describe the design principles of the flow reactor followed by the experimental details of the entire reactor system. The underlying goals of the flow reactor design are the elimination of wall interference, the reproducibility of the experiments, and the control over and ease of changing experimental conditions.

### 3.1 Reactor Design Principles

A flow reactor inherently allows rapid change in experimental conditions since the reacting mixture is flowing through the tube continuously. Provided the reactor gives reproducible results, one is limited only by the residence time in the irradiated section and the gas handling and flow development time. The reproducibility of the reactor is assured if the walls play no measurable role in the results. This is assured if any product buildup on the walls is negligibly small and does not affect the measurements. Thus a fundamental goal in the design and operation of the Science Center flow reactor is to prevent the walls from playing any role in the reactions studied. In order to achieve this, one must analyze the possible effects of having a finite volume reactor. In a static chamber the known interferences are removal of reactants and products by the walls and the contamination by sources at the walls. Both these effects are limited by diffusion so one can hope to reduce the effects of the walls by increasing the volume to surface ratio of a chamber. However, in most experiments, samples must be physically removed from the chamber for analysis. In this case the "static" chamber is no longer static and mixing is required to keep it homogeneous. A flowing reactor solves this type of sampling problem and does not have to be mixed to remain homogeneous. Diffusion to and from the walls remains the limiting interference problem. In a fully developed laminar flow there is no eddy diffusion so only the much slower molecular and Brownian diffusion must be considered. We will now discuss these diffusion problems as they affect a fully developed laminar flow reactor in which chemical reactions are taking place and in particular in which aerosols are formed.

In order to understand diffusional problems in a chemical flow reactor

we must consider both loss of material and appearance of interfering substances. Each of these cases has subcases. The loss of an initial reactant will lead to an apparent increase in its reaction rate, while the loss of a product will lead to an apparently lower formation rate. In the latter case, gas phase products may be lost to the walls by molecular diffusion as in the case of loss of reactants, but aerosols may be lost by the analogous Brownian diffusion and also by gravitational settling. For the interference case the appearance of contaminants from the wall may produce new products not otherwise obtained from the experimental reacting mixture, or the contaminant may react with and remove an initial reactant, a product, or a key intermediate. In the sub-case of removal, the result may be an apparently faster or slower reaction rate but it may also be the insidious removal of an intermediate by reacting it to an otherwise present species. This kind of an interference would be almost impossible to detect but could dramatically change the experimental results. These various cases are summarized in Table 3.

All of these cases, except for gravitational settling of aerosols, are described by the following partial differential equation for diffusion in a steady flow:[31]

$$v(r)\,\frac{\partial C}{\partial z} = \frac{D}{r}\,\frac{\partial}{\partial r}\left(r\,\frac{\partial C}{\partial r}\right) + R(C,r,z) \qquad (1)$$

where $C = C(r,z)$ is the concentration of the species in question

$D$ is its diffusion coefficient in air

$r$ is the radial position

$z$ is the axial position

$v(r)$ is the mean velocity (in z direction only for laminar flow)

$R$ is the chemical rate of production or removal of species in question.

In general this equation cannot be solved in closed form due to the non-linearities introduced by the term $R(C,r,z)$. In fact for the typical case in question in this program, this nonlinear term couples the equation to a large set with one equation for each species. However if $R = 0$ or is linearly dependent upon $C$ (i.e. $R = \pm kC$), then equation (1) separates into

Table 3

Wall Interference in the Flow Reactor

1. Loss to the Walls*

   A. Diffusional loss of initial reactant leading to apparent higher reaction rate.

   B. Loss of product leading to apparent lower formation rate.

      1) Diffusional loss of gas phase molecules

      2) Brownian diffusional loss of aerosols

      3) Gravitational sedimentation of aerosols

2. Diffusion Contamination from the Walls*

   A. Appearance of material which produces contaminant products.

   B. Appearance of material which reacts to remove key reactants and intermediates.

*Note: A reaction catalyzed at the walls falls simultaneously in both 1 and 2. The catalyzed reactants are lost and the products formed represent a contaminant source.

an equation for the z dependence and one for the r dependence. In both cases the z equation has a simple solution. The r equation depends upon the factor v(r). If it is constant, $v(r) = v_o$, then the resulting r equation is Bessels equation of order zero.[32] If v(r) represents laminar flow, that is $v(r) = v_o(1 - \frac{r^2}{a^2})$, where a is the radius of the tube, then the r equation may be reduced to the Confluent Hypergeometric Equation.[33] It has been shown that for a flow reactor assuming that $v(r) = v_o$ only results in a small change in the solution for the case of R = 0.[32]

In order to simplify the analysis of the wall problems we will make some extreme simplifications of the problem to keep R = 0. These will represent "worst cases" and will not be physically realizable. However we will then be assured that the true problem is considerably less important than the calculated one. Since for many of the entries in Table 3 the wall effects will be unimportant, these overstatements of the problem will be totally satisfactory. For the cases in which the wall effects produce limitations, the stringent nature of the "worst case" assumptions must be kept in mind.

For case 1(A) we will assume that the reactant must be present during the entire residence time, but that it is trapped at the walls. In other words it will be diffusing away for the entire residence time but its presence as a reactant is most important at the end of the period. On the other hand for 1(B) cases we will assume that the product is formed immediately and has the remainder of the time to decay. Of course, if such a product is other than an intermediate posing as a case 1(A) reactant, then the residence time would just be made shorter. For subcase 2 we will assume that the aerosol consists of a very small nuclei which only have an effect near the end of the time while for subcase 3 we assume the aerosol has grown to be very large initially. For both cases 2(A and B) we will assume a source at the wall such that the concentration at the wall is comparable to the other important intermediates or aerosol precursors but that it does not have an effect until it reaches the end of the residence period. Now with these assumptions we may quantitatively explore the limitations of the flow reactor. These are highly unrealistic cases so the solutions will be bounds on the

true behavior in the flow reactor. In some cases the change to more realistic assumptions will be easy; in many, however, this represents a difficult problem.

Once R has been taken as zero and $v(r) = v_o$, equation (1) may be separated and solved exactly. One obtains[34]

$$C = \sum_{n=1}^{\infty} A_n J_o(\alpha_n r) e^{-D\alpha_n^2 t} \tag{2}$$

where $J_o(x)$ is the zero order Bessel function $a\alpha_n$ is the zero of $J_o$ (i.e. $J_o(a\alpha_n) = 0$ and the $A_n$'s are to be determined by the boundary conditions, and the variable z has been replaced by t such that $z = v_o t$.

For case (1) we have as boundary conditions

$C = 0$ for $r = a$ and $t > 0$

$C = f(r)$ for $t = 0$ and $0 < r < a$

Now the solution is[34]

$$C = \frac{2}{a^2} \sum_{n=1}^{\infty} e^{-D\alpha_n^2 t} \frac{J_o(r\alpha_n)}{J_1^2(a_n)} \int_o^a r\, f(r) J_o(r\alpha_n) dr \tag{3}$$

The solution consists of a sum of modes determined by the zeros of $J_o$. Since $\alpha_n$ increases rapidly from one zero to another and we will see that $D\alpha_1^2 t$ is already appreciable, then in a reasonable time all the higher modes will drop out and only the $\alpha_1$ mode will remain. Thus for case 1(A) we will assume that when the flowing mixture enters the irradiated portion of the reactor, its initial distribution is given by $f(r) = C_o J_o(r\alpha_1)$. Equation (3) now reduces to

$$C = C_o J_o(r\alpha_1) e^{-D\alpha_1^2 t} \tag{4}$$

The first root of $J_o$ is at $a\alpha_1 = 2.405$ and a is taken to be 2.5 cm for now. D will range from 0.05 $cm^2/sec$ for a typical small organic molecule[36] to

0.282 for $H_2O$[35] all in air at STP. On the axis (r = 0) $J_o = 1$ so $C/C_o = e^{-D\alpha_1^2 t}$. Thus for a one second residence time the loss ranges from 4.5% to 23% for the range of D specified. The loss is sharply dependent upon the residence time growing to 21% for D = 0.05 and 5 second residence. However for increasing diameter the improvement is dramatic since $\alpha_n$ is inversely proportional to $a^2$. Thus for D = 0.282, t = 1 second, and a = 5 cm, the loss drops to 6.3%. A series of these results are summarized in Table 4. Once again it must be noted that the assumption of total adsorption at the walls is stringent for our experiments. The solution of the equations becomes more complex for all other cases, except that of no adsorption, in which case diffusion has little effect.

Case 1(B.1) is somewhat more complicated than 1(A). If the product is formed in a reaction dominated by a reactant which is adsorbed at the wall, then it will be produced with an initial distribution proportional to $J_o(r\alpha_1)$ and the solution will be the same as that above. On the other hand if the product is formed by a group of reactants uniformly distributed (i.e. no adsorption at the wall for reactants) then higher modes ($A_n \neq 0$, $n > 1$) must be included. Since the $\alpha_n$'s increase rapidly with n the higher modes will damp out quickly. For example, if the first mode has a 10% loss for a given case, the next mode will have a 43% loss and the third mode a 74% loss. For the initially uniform case the first mode will represent only 67% of the sum and the remainder of the terms will oscillate in sign making approximate solution difficult. Thus we conclude that for a product initially uniformly distributed and with a moderately large diffusion coefficient the higher modes will all be lost so a loss of 33% must be added to those estimated above. Fortunately the types of products which will accumulate in aerosols will be much larger molecules and have small diffusion coefficients, but it is certainly true that such products will be adsorbed on the walls.

Although the losses to the walls for extreme cases can be large, this is not a serious defect in a flow reactor as long as the reactions being studied are not too much slower than the rate of loss to the walls. Even for very accurate rate measurements such losses are regularly accounted for in measurements of rate constants in flow reactors.[32,33]

Table 4

DIFFUSIONAL LOSS IN A FLOW REACTOR
(See text for symbol definitions)

| $D^{\ddagger}$ | a | t | C/Co | Loss |
|---|---|---|---|---|
| $cm^2 sec$ | cm | sec | - | - |
| 0.282 | 2.5 | 1 | 0.7703 | 23% |
| 0.05 | 2.5 | 1 | 0.9548 | 4.5% |
| 0.282 | 2.5 | 5 | 0.2712 | 73% |
| 0.05 | 2.5 | 5 | 0.7935 | 21% |
| 0.282 | 5 | 1 | 0.9368 | 6.3% |
| 0.05 | 5 | 1 | 0.9885 | 1.2% |
| 0.282 | 5 | 5 | 0.7216 | 28% |
| 0.05 | 5 | 5 | 0.9438 | 5.6% |

$^{\ddagger}$Note D = 0.282 represents $H_2O$ in air at 1 atm and 16°C[35] and D = 0.05 is a typical ion molecular weight hydrocarbon in air at STP.[36]

For case 1(B.2) the Brownian diffusion of aerosols, the molecular calculations can be carried over exactly. For our calculations however we have gone to the aerosol literature directly for the required solutions. We find that for laminar flow in a tube,[37]

$$\bar{n}/n_o = 1 - 2.56\mu^{2/3} + 1.2\mu + 0.177\mu^{4/3} \qquad (5)$$

where $\bar{n}$ is the mean number of aerosol particles at the end of a tube

$n_o$ is the number at the entry to the tube

$$\mu = \frac{DL}{R^2\bar{u}} \qquad (6)$$

where D is again the diffusion coefficient

L is the length of the tube

R is the radius of the tube

$\bar{u}$ is the mean velocity of the flow

This solution is valid for small $\mu$ which is applicable to aerosol behavior.

If we now define the axial residence time T as:

$$T \equiv \frac{L}{2\bar{u}} \qquad (7)$$

so that combining equations 6 and 7:

$$T = \frac{R^2\mu}{2D} \qquad (8)$$

If we now take $\bar{n}/n_o = .99$ and solve equation 5 for $\mu$, we find $\mu \cong 2.5\times10^{-4}$. For our reactor R = 2.5 so $T = 1.95\times10^{-3}/D$. To find D we note that

$$D = k\tau B$$

where k is the Boltzman constant

$\tau$ is the temperature in °K

B is the mobility

The mobility is given by

$$B = \frac{(1 + A\frac{\ell}{r} + Q\frac{\ell}{r}e^{-br/\ell})}{6\pi\eta r} \qquad (10)$$

where $\eta$ is the viscosity of the medium

$\ell$ is the mean free path of molecules of the medium

r is the radius of the particle

A, Q, and b are constants with values

A = 1.246, Q = 0.42, b = 0.87

For 0.01 $\mu$ radium particles in air at STP, $B = 3.4\times10^{9}$ so $D = 1.41\times10^{-4}$ giving T = 14 sec which means in 14 seconds only 1% of the 0.01 $\mu$ radius particles will be lost.

Particles may also be lost by gravitational settling. Similarly to the above a standard expression is also extracted from Fuchs.[38] Since it is unlikely that this would be a problem, we will just state the result here for completeness. For a 1% loss under the same conditions as in the diffusion cases and for 0.1 $\mu$ particles we will have a residence time of 650 sec.

Now we move on the cases 2(A and B) which quantitatively we can treat together. Once again the solution is equation (2) but with new boundary conditions.

$C = C_o$ for $r = a$ and $t \geq 0$

$C = 0$ for $t = 0$ and $0 < r < a$

The solution satisfying these boundary conditions is[34]

$$\frac{C}{C_o} = 1 - \frac{2}{a}\sum_{n=1}^{\infty} e^{-D\alpha_n^2 t}\frac{J_o(r\alpha_n)}{\alpha_n J_1(a\alpha_n)} \qquad (11)$$

This solution can be expressed in terms of two dimensionless parameters $Dt/a^2$ and $r/a$. Curves of $C/C_o$ versus $r/a$ for various values of $Dt/a^2$ have been presented by Crank.[34] For $C/C_o = 0.01$ and $v = 0$, $Dt/a^2 \simeq 0.05$ so we have

$$t = \frac{0.05a^2}{D}$$

for our range of D from 0.05 to 0.282 and for a = 2.5 cm we find residence times of from 6 secs down to 1 second. Again, it must be noted that this is a restrictive calculation. Any product molecule large enough to be important in aerosol formation probably has a smaller diffusion coefficient than that of our present range so less of it will reach the detector. More important is the fact that if the product diffusing from the walls is sufficiently important in producing aerosols it will have so reacted on its way from the wall to the detector forming an aerosol which has a much lower diffusion rate. Thus the figures above are really for gas phase contaminants and in the case of aerosol production, or for that matter inhibition, they are more limiting than necessary. Nevertheless for the feasibility study described in this report, these contamination calculations were considered to be the limiting case, for if results can be obtained with these limitations, then relaxing them will only make the experiments easier.

The above discussion assumes a non-turbulent flow in the reactor. Two conditions are required for such a flow. The Reynolds number for the flow must be sufficiently small and the flow must have a certain distance over which to develop. The Reynolds number for flow in a tube is given by,

$$R = \frac{a\rho v}{\eta} \qquad (12)$$

where a is the radius

$\rho$ is the density

v is the average velocity

$\eta$ is the viscosity.

Since for laminar flow the velocity on axis is twice the average velocity $v = \ell/2t$ where $\ell$ is the length of the reactor, t is the residence time on the axis then:

$$R = \frac{a\rho\ell}{2\eta t}$$

Now for air at STP

$$\rho = 1.2\times10^{-3} \text{ gms cm}^{-3}$$

$$\eta = 1.845 \text{ poise (gms cm}^{-1}\text{sec}^{-1})$$

and if we take a = 2.5 cm, $\ell$ = 20 cm, t = 1 sec, which represents our reactor,

$$R = 163$$

which is well below any critical Reynolds number.

For development of laminar flow a length $\ell_e$ is required given by

$$\ell_e = 0.227\ aR$$
$$= 92 \text{ cm}$$

So the conditions of laminar flow are easily established in a laboratory flow reactor at STP.

It is interesting to explore how these quantities vary with changes in reactor size and residence time. We noted above that for a given diffusional contamination from the wall

$$t = \gamma a^2$$

where $\gamma$ is some constant. Thus, if we want to keep this criteria the same we may increase the time by the square of the increase in the radius.

Our expressions for R and $\ell_e$ now become (on substitution for t)

$$R = \frac{\rho \ell}{2n\gamma a}$$

$$\ell_e = \frac{0.277\ \rho \ell}{2n\ \gamma}$$

so the Reynolds number becomes smaller and the flow development length remains the same. One can also examine the quantity of gas consumed for a larger reactor. The quantity of gas flow Q is given by

$$Q = \frac{\pi a^2 P \ell}{t}$$

where a, $\ell$, t are as previously defined.

P is the mean pressure but for $t = \gamma a^2$

$$Q = \frac{\pi \ell P}{\gamma}$$

which is independent of reactor diameter.

Thus one can quite dramatically increase the residence time without cost in quantity of gas or length of flow development. However as the radius becomes larger, care must be taken to keep the reactor isothermal since thermal convection could disrupt the laminar flow.

## 3.2 Detailed Description of Experimental System

The experimental system is composed of the flow reactor with its irradiated section, a gas handling system, and a sampling and measuring system. A schematic drawing of the flow reactor, gas handling, and sampling systems used in this study of aerosol formation is shown in Figure 3. Figure 4 is a photograph of the system. A high degree of flexibility, afforded by

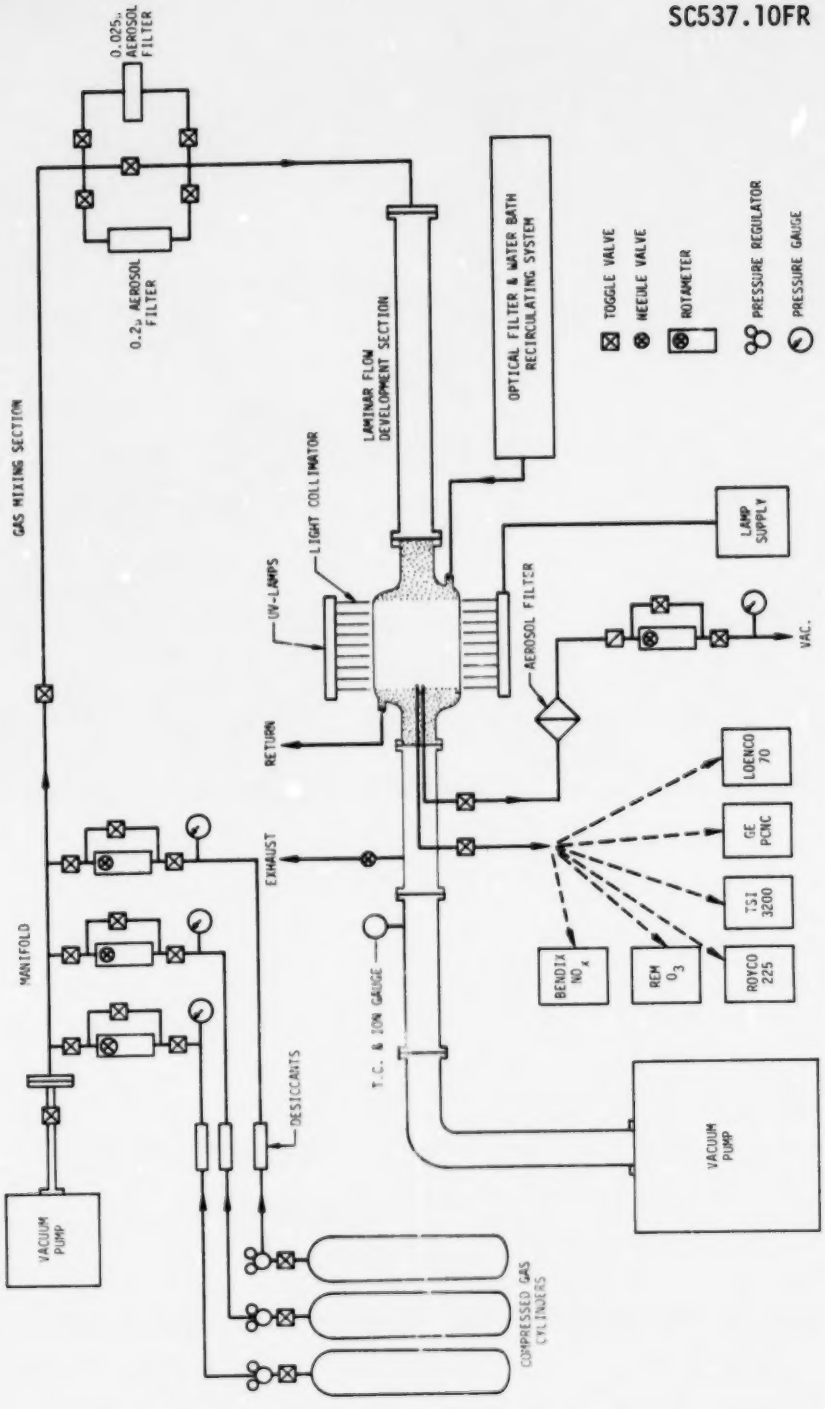


Figure 3 SCHEMATIC DIAGRAM OF THE SIMULATION REACTOR SYSTEM

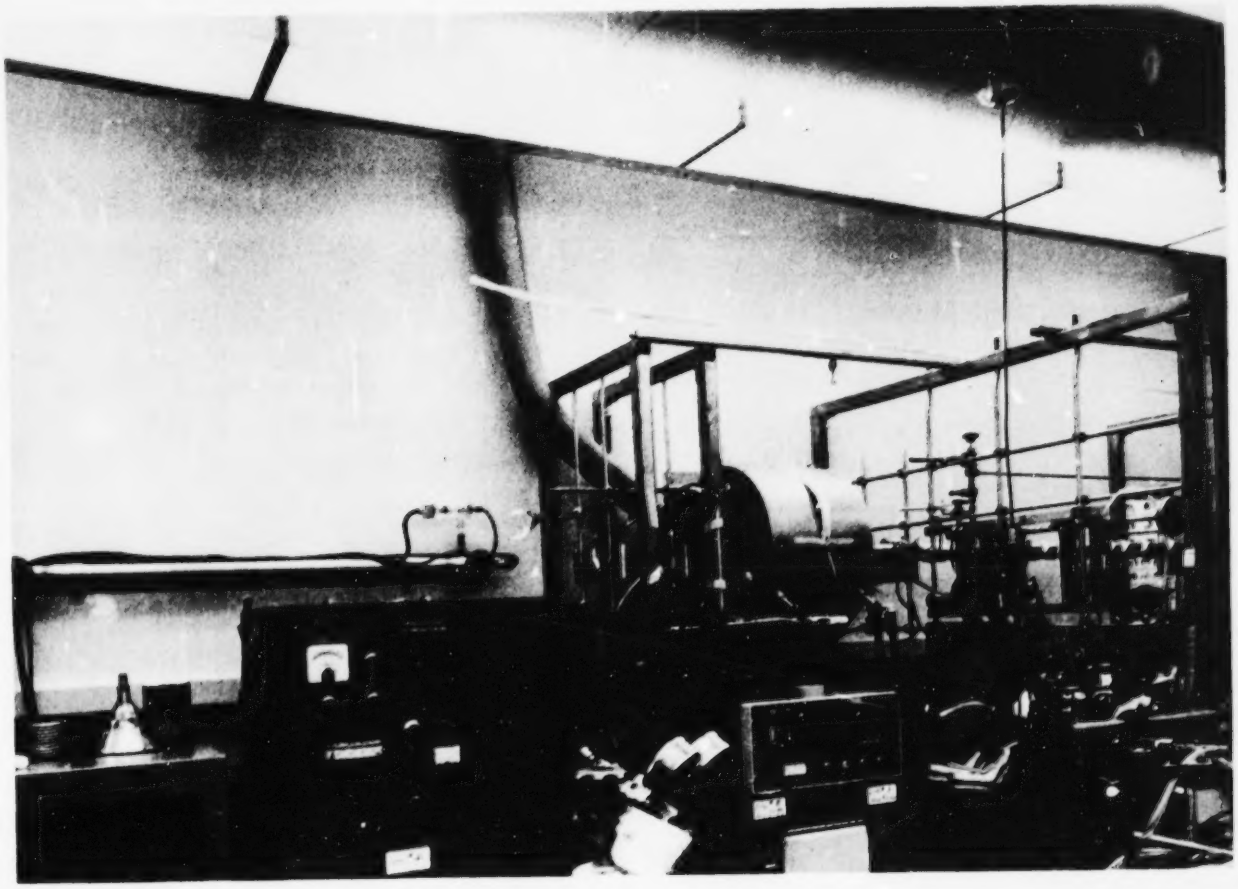

Figure 4. PHOTOGRAPH OF THE PHOTOCHEMICAL AEROSOL REACTOR LABORATORY

utilizing a modular concept for the overall design, allows a variety of changes in gas handling, flow rates, sampling methods, among others. We will now describe the design and operation of the individual components of the system.

3.2.1 The Reactor Section. Central to our entire experiment is the reactor section itself. The gas mixture enters the reactor through the laminar flow development section, a 5 cm diameter, 180 cm long stainless steel tube. The dimensions of the tube are more than adequate for the development of laminar flow at our operating conditions, of a total flow of less than five liters per minute (see sec. 3.1). The reactor itself is a single unit of pyrex glass tubing, 5 cm diameter and 20 cm long, surrounded by a torroidal jacket which contains a temperature controlled light filtering solution.

The spent gas that has gone through the reactor is then vented into the exhaust system. A diaphragm indicates the pressure differential between the reactor and the ambient and a needle valve controls the vent rate and therefore the pressure.

3.2.2 Gas Handling. Input to the reactor system is from a series of flow control devices and filters which prepare the gas mixture in the desired concentrations. The dry air is reconstituted from the laboratory central supply of oxygen and nitrogen. The oxygen is supplied in tanks from Airco. The nitrogen is obtained from the boil off from liquid nitrogen which is also supplied by Airco. The oxides of nitrogen and hydrocarbons are obtained as mixtures of an individual component in nitrogen from Matheson. Typically these are 2000 ppm but for some of the hydrocarbons like 1-hexene it was 800 ppm. The $SO_2$ was also obtained mixed with $N_2$ at 800 ppm supplied by Linde. Water vapor was added by diverting a part of the nitrogen flow through a bubbler which saturated it with water. For higher molecular weight hydrocarbons a temperature controlled saturator has been constructed. In order to perform experiments without water vapor present the individual gases were passed through dessicants. For $N_2$, $O_2$, and NO, molecular-sieve was used and for olefins and $NO_2$, magnesium perchlorate was used. Six sets of rotameters, pressure regulators and valves serve to define and measure the flow-rate and pressure. Each rotameter with its own pressure regulator and pressure gauge

is calibrated, in the system, with a Precision Scientific wet test meter or a soap bubble meter depending on the flow rate of interest. The flow rates of the individual gases not only determine the concentrations but also reactor residence time.

From the manifold, through the mixing section, the blended gas stream is then filtered to remove any residual aerosol. Two filters were used and were tested for effectiveness: a Gelman membrane filter capsule with a mean pore size of 0.2μm and a Millipore mixed ester of cellulose with a mean pore size of 0.025μm. The General Electric portable condensation nuclei counter indicated low level of background aerosol count ($\lesssim$ 300 counts/cc) with or wthout these filters suggesting residual aerosol content in the blended gas is minimal compared to reactor generated aerosol count. Most of the experiments were carried out without these filters.

The whole reactor system, including the gas handling system up to the desiccants, can be evacuated. Two high vacuum pumps are used, one upstream of the manifold and the other downstream of the reactor section. This arrangement provides fast pumping speeds as well as flexibility in evacuating the flow section or the gas handling section separately. Finally, in one sampling configuration, the sampling probes themselves can be vacuum cleaned after each sampling cycle to remove any residual contaminants left there from a previous run. During the set of experiments described in Sec. 4.1.2, the system was found to be reproducible, after complete evacuation, for the duration of the G.C. measurements.

3.2.3 Irradiation. Three Hanovia 674-A medium pressure mercury vapor lamps, axially arranged in an aluminum housing, provide UV radiation for the flow reactor. Table 5 gives the approximate radiated energy in watts for several strong mercury lines in the spectral region of interest between 2900Å and 5000Å.

The light from the mercury lamps is collimated by a series of 14 washer-like disks or baffles establishing a radiation zone with abrupt edges (see Fig. 3). Any part of the glass reactor not in the radiation zone is painted black to prevent light leaks. The glass probes are wrapped with black tape,

Table 5

SPECTRAL ENERGY DISTRIBUTION IN THE REGION OF INTEREST

| Mercury Lines (angstroms) | Radiated Energy (watts) |
|---|---|
| 5461 (green) | 34.0 |
| 4358 (blue) | 29.0 |
| 4045 (violet) | 15.9 |
| 3660 (UV) | 40.5 |
| 3341 | 3.8 |
| 3130 | 21.0 |
| 3025 | 11.3 |
| 2967 | 6.5 |
| 2894 | 2.3 |

thus defining precisely the boundaries of the reaction zones and the residence time of the reactor. Figure 5 shows a photodiode measurement of the relative light intensity on axis from each of the three lamps.

After the radiation is collimated, it is then filtered as it passes through the torroidal jacket around the reactor. The transmitted spectral characteristic is determined by the optical filter used. The pyrex glass of the reactor itself cuts off at about 2900Å thus eliminating the hard ultra-violet. Cobalt sulfate or cobalt chloride solutions can be used as bandpass filter from about 3000Å to about 5000Å. Cupric sulfate solution gives a sharp cut off at the short wavelength side of about 3200Å. Aquadag is used as a neutral density filter and its spectral characteristic is essentially flat. The approximate light intensity, in terms of the dissociation of $NO_2$, is estimated to be a minimum of $kd = 0.02\ sec^{-1}$. The difficulties in arriving at it are discussed in section 4.1 below.

3.2.4 Sampling. In analyzing the chemical and physical characteristics of the reaction products, two types of samplers were used: a) grab samplers and probes, which are defined as devices employing relatively short accumulation times and b) collectors or filters, which require much longer sample accumulation times. Sampling of all gas phase components for chemical analysis and aerosols for physical characterization were done with probes and devices for obtaining grab samples. Since dark reactions occur in the short time required for the material to travel from the tip of the sampler to the specific analyzer, probes must either eliminate or allow measurement of this effect.

Another constraint on the design of the sampling devices is the limitation of the specific analyzer detection range. Some of the analyzers were designed and built as air monitoring instruments and not as laboratory instruments required to measure trace gas concentrations much higher than ambient. They often also require high flow rates compared with what we needed for isokinetic sampling. The sampler therefore must incorporate some sort of dilution system.

Figures 6 and 7 show the first model dilution probe. The arrows indicate

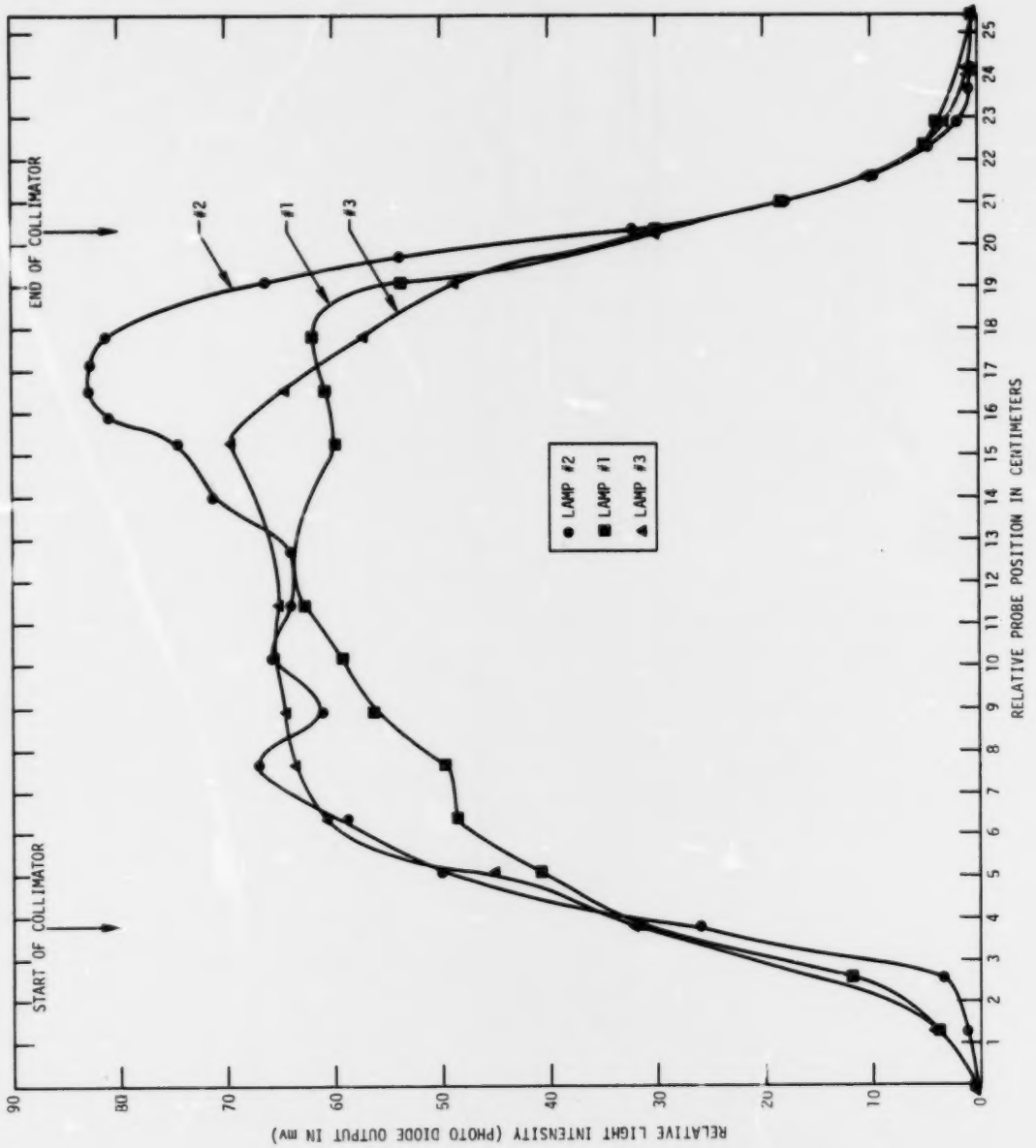


Figure 5 PHOTODIODE MEASURES OF THE RELATIVE LIGHT INTENSITY OF THE THREE UV LAMPS

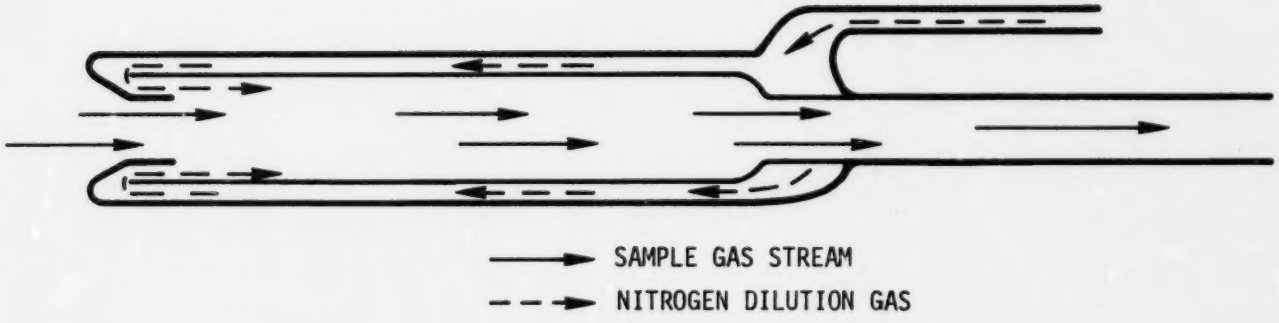


Figure 6 SCHEMATIC DRAWING OF SAMPLING PROBE (DILUTION PROBE #1)

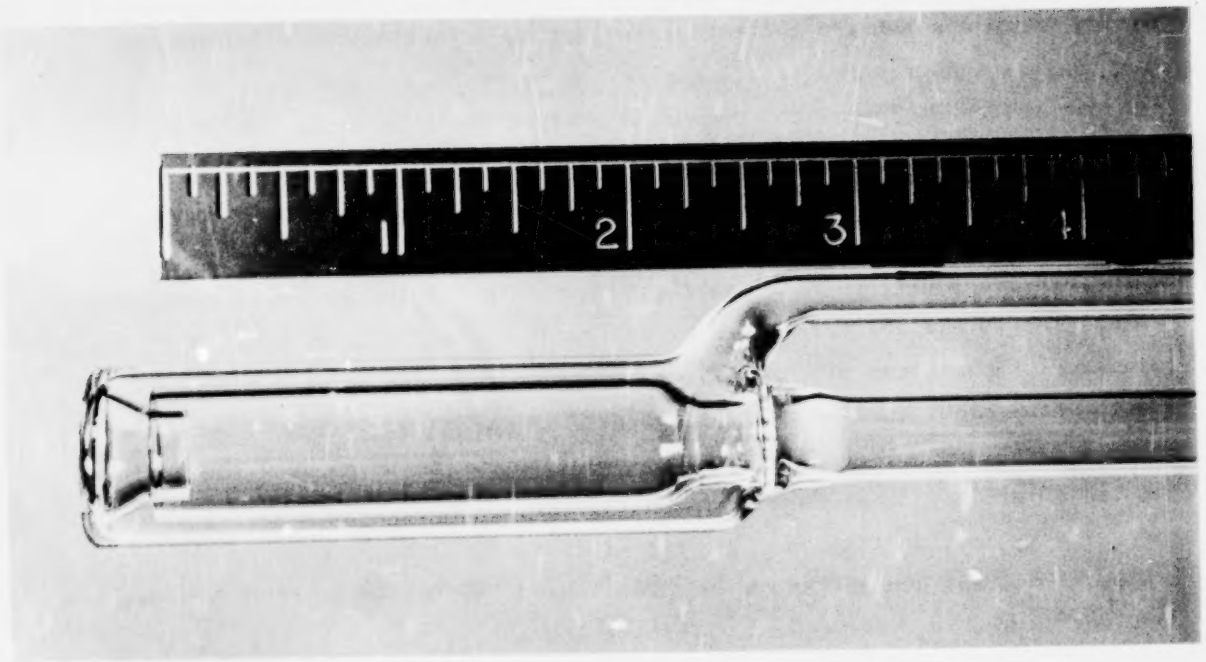


Figure 7. PHOTOGRAPH OF SAMPLING PROBE (DILUTION PROBE #1)

the diluent (dry nitrogen gas) flows to the tip of the sampling probe on the outside jacket and is injected into the sample stream diluting it and carrying it to the analyzers. By varying the length of the teflon tubing, joining the probe and and the analyzers, and by adjusting the dilution rate, dark reactions during the sampling time can be minimized and measured.

Figures 8 and 9 show the second generation dilution probe operating on the same principle except that the dilution gas flows to the probe tip through the center glass tube and is injected into the sample gas stream through the six holes located on the back side of the arrow shaped Teflon tip. This probe differs from the first in that not only can grab samples be transported to the analyzers with minimized dark reactions but dark reactions immediately downstream of the reactor radiation zone can be measured at those reactor flow conditions as well as the dark reactions occurring between the probe and the analyzers. The center glass tube can be moved back thus delaying the dilution process further downstream in the probe and creating a longer dark reaction time near the tip of the probe (slower flow rate) at a higher reactant concentration (no dilution). This variability effectively provides us with another piece of information on the faster initial dark reactions at relatively higher reactant concentrations. Some of the results are discussed in section 4.1. The residence time in the irradiated section can be varied from zero to the maximum, as defined by the total flow rate through the radiation zone, by simply changing the probe position within the reactor.

The chemical characterization of the aerosol requires the use of filters and extremely long collection times. The choice of filter is based on several considerations: (a) reaction conditions, i.e., materials and flow; (b) collection efficiency and mesh size for the smallest size range of interest; and (c) the ability of the filter paper to withstand chemical reagents during the analytical process. For examples, Whatman filters have a particularly high affinity for water adsorption. Gelman glass fiber filters are very fragile tending to lose weight in handling but it can withstand elevated temperatures and strong chemical reagents. Millipore cellulose papers have pore size ranging down to 0.025 μm but are susceptible

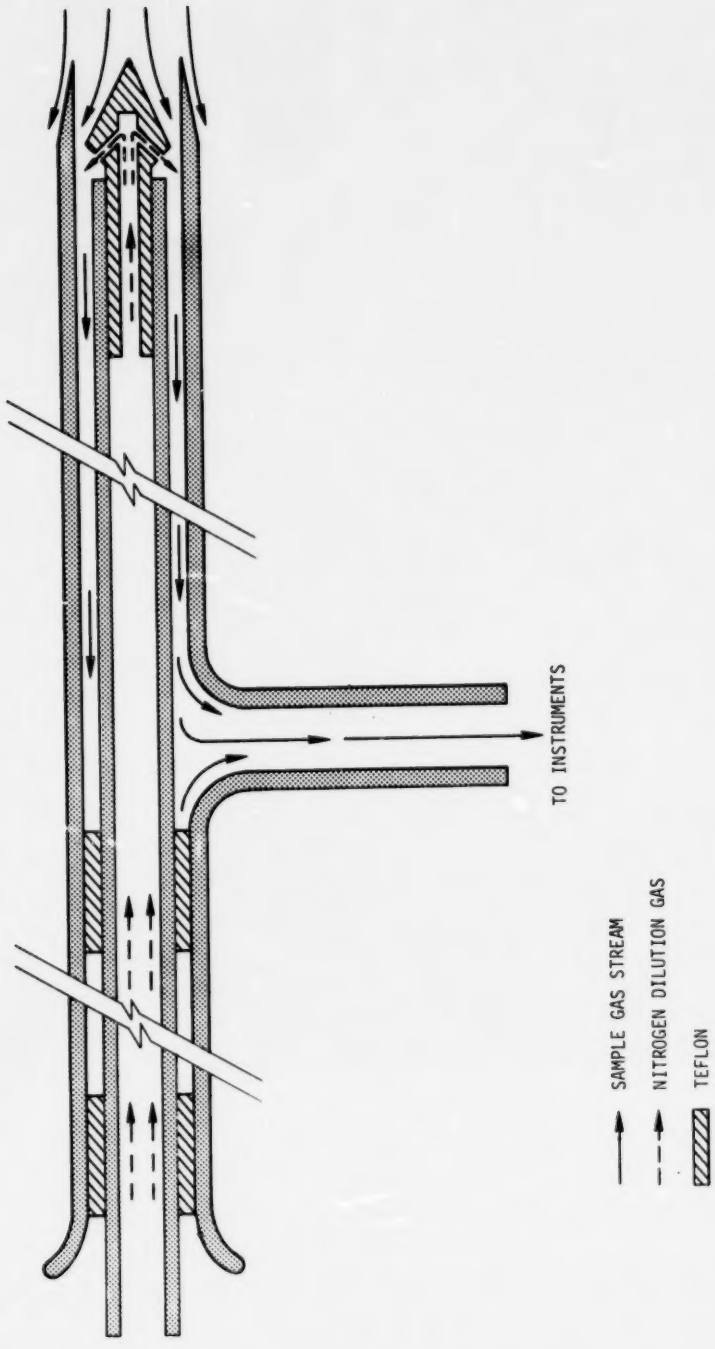


Figure 8 SCHEMATIC DRAWINGS OF SAMPLING PROBE (DILUTION PROBE #2)

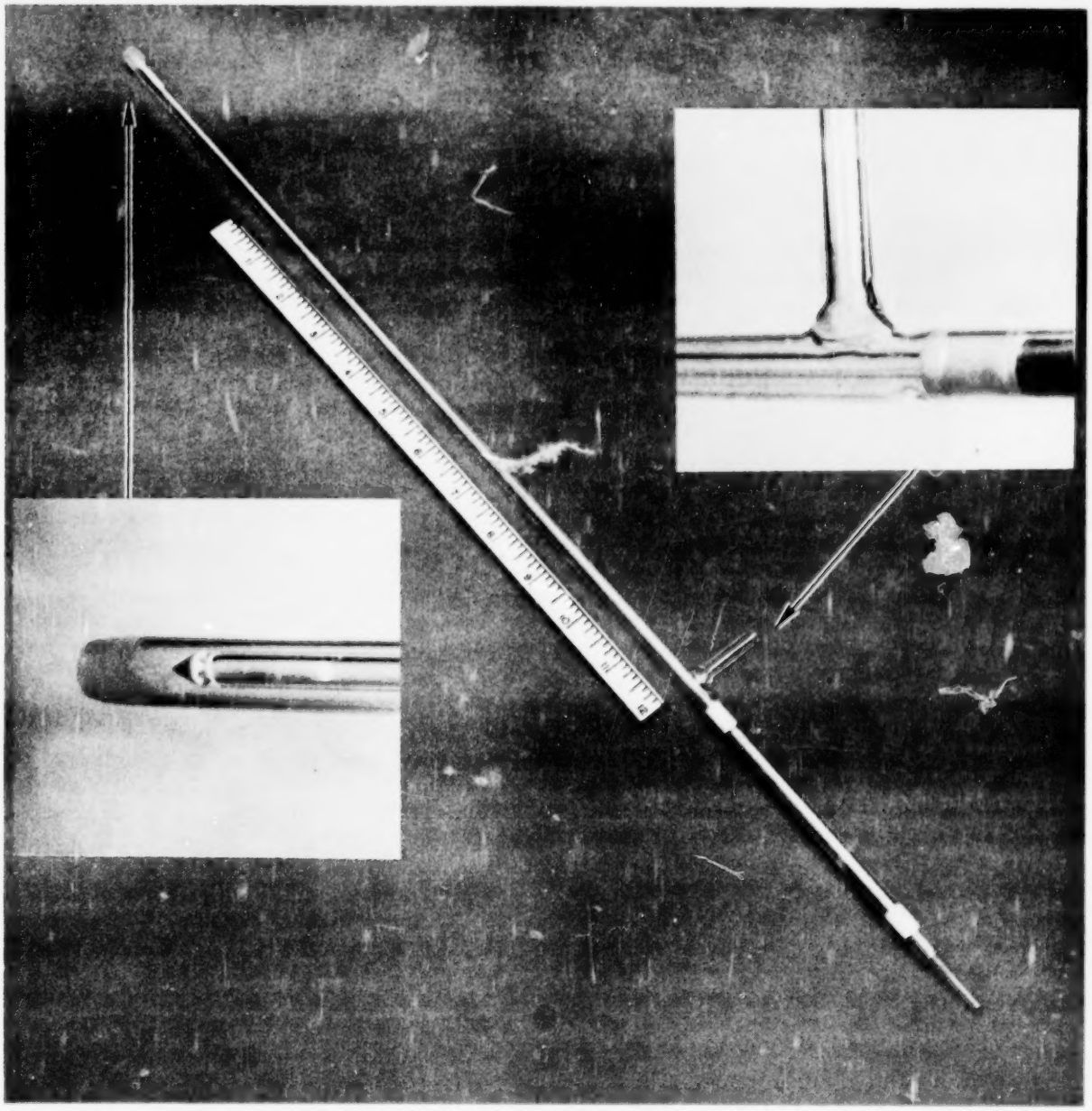

Figure 9. PHOTOGRAPH OF SAMPLING PROBE (DILUTION PROBE #2)

to damage in some chemical reagents such as isopropyl alcohol. Nuclepore filter seems to suit many needs: (a) it has a well defined pore size and pore shape, (b) it is chemically inert to many solvents, strong acids, and bases, (c) it is extremely hydrophobic, and (d) the filter itself is strong and can withstand repeated handling. However, the Nuclepore filter cannot be elevated to extreme temperatures. We have used primarily the Gelman glass fiber filters and the Nuclepore filters.

### 3.2.5 Measurement Techniques

#### Gas Phase Analyzers

For the inorganic analysis standard chemiluminescent instrumentation was employed in order to save the time of special instrument development. As indicated above, this created sampling problems and in addition extensive warranty servicing was required to bring them up to specifications initially. Overall these instruments save some time and effort; it was not as great as we expected. For ozone, a REM model 612 chemiluminescent detector was employed, and for $NO_x$, a Bendix $NO\text{-}NO_2\text{-}NO_x$ Analyzer was employed.

In the gas phase analysis of organic reaction products, the Loenco model 70 Hi-Flex Gas Chromatograph with hydrogen flame ionization detector, helium carrier gas, was used. Retention time analysis and peak identification are discussed further in section 4.1.2.

#### Physical Measurements of Aerosols

Three particulate monitoring instruments were used for the detection and characterization of aerosols generated in the simulation reactor. The instruments are: a condensation nuclei counter, a total mass monitor, and an optical analyzer for larger size particles.

The condensation nuclei counter used in the General Electric model PCNC-1 which detects a total number of particles nominally in the 0.005 to 0.1 μm diameter size range. It can detect as few as ~ 300 particles per cc and up to ~ $10^7$ particles per cc. The instrument sampling rate is two cycles per second with a sample flow rate of 20 cc per second. The PCNC was not well calibrated since only an order of magnitude indication was used.

For the larger size aerosol particles, the Royco 225 optical counter measures particles in four ranges from 0.5 to 5 μm diameter. However, this particular

instrument suffers from an inherent drawback of a lack of resolution near 0.3 μm diameter associated with the geometry of the light scattering cell and unusual high background noise level. Within the limited resolution of this instrument, optical-size aerosol concentration was observed to be less than a few particles per cubic centimeter. It is anticipated that the newly acquired Royco 220 interfaced with a multi-channel analyzer will improve size resolution as well as lower noise background.

Total aerosol mass concentration of particles of size from 0.01 to 10 μm in the range of 1 to 100,000 $\mu gm/m^3$ can be measured on the Thermo Systems, Inc. system 3205. Time resolution of this instrument is one second, although best results are obtained for the lowest concentration range and for long integration periods of 100-200 seconds. Supplemental to the mass monitor, the weighing of filter samples over a period of collection time is also employed. The filter samples, however, were more important in the analysis of aerosol chemistry.

## 4. Experimental Results and Discussion

Since the entire reactor concept was novel and we anticipated certain limitations and potential difficulties, moderate effort was devoted to checking the gas phase reactions in the flow reactor. Due to limitations of time these were not as extensive as they must ultimately be in order to fully understand the reactor and its operation. They were carried forward to the point that we had a qualitative understanding of the data which was sufficient to allow aerosol experiments. We will now discuss these experimental tests and the conclusions reached.

In the second part of this section we will discuss the aerosol experiments including both the aerosol production tests and the collection and chemical analysis of the aerosols produced.

### 4.1 Gas Phase Chemistry

4.1.1 Inorganic Gas Phase Tests. The first experiments performed to test the flow reactor were the measurements of ozone production in the photolysis of $NO_2$ in air. The choice of this system was determined by the availability of the REM ozone monitor and the difficulties experienced with the Bendix $NO_x$ monitor. Later we studied the simpler photolysis of $NO_2$ in $N_2$.

Using the REM instrument, ozone was measured in the flow reactor with an $NO_2$ concentration of 20 ppm. The ozone concentration as measured was only approximately 5 pphm. In addition the ozone concentration was found to decrease with increasing light intensity. At this point the dilution probe #1 was employed to check the effect of dark reactions on the measurement of ozone. It was found that for increased dilution the measured ozone concentration increased, indicating that dark reactions were important. The dilution effect however could only be fitted quantitatively by assuming the concentration of NO was considerably higher than the $O_3$, at the sampled point, in the reactor. This is not inconsistent with the decrease in ozone with light intensity and suggests that competing reactions of O atoms with $NO_2$ were producing NO. Further tests with a telescoping hood on the probe to increase dark reaction time, supported this possibility but at the same

led to the design of the second dilution probe.

These data suggest that there would be a peak in the ozone concentration as a function of the $NO_2$ concentration. The peak was found at about 5 ppm of $NO_2$ and was about 12 pphm of ozone (at the REM). Under these conditions the ozone concentration increased with light intensity, but this dependence was very nonlinear, with a 10% increase in ozone concentration for double the light intensity.

While all these observations formed a consistent picture in terms of qualitative behavior, the quantitative measurements were inconsistent. The peaks in ozone as a function of $NO_2$ concentration and light intensity should have occurred at values of these parameters 10 times those observed. At these levels the ozone concentration would be comparably higher. From the measured ozone concentration a value of kd for $NO_2$ of about 0.02 $sec^{-1}$ could be estimated while for the presence of the peaks in ozone concentration values from 0.06 $sec^{-1}$ to 0.5 $sec^{-1}$ would be required.

In order to clarify this, and with the availability of the Bendix instrument, the dissociation of $NO_2$ in $N_2$ was measured. In this case the concentration of NO reached an equilibrium value after traversing about 1/3 of the illuminated region (8 cm). The slope in the linear region of variation of NO concentration with light intensity indicated a value of kd of about 0.01 $sec^{-1}$ while the occurrence of an equilibrium required a value of the order of 0.3 $sec^{-1}$.

These discrepancies remain a problem in the interpretation of the experiments performed in the reactor.

Although uncertainty exists about the level of the light intensity in the reactor, it is great enough to produce appreciable quantities of ozone. At this point due to time requirements and the feasibility nature of the study, as well as the fact that the aerosol production was of utmost importance, it was decided that the completed work on the inorganic reactions was sufficient to allow some aerosol formation experiments. In addition, improvements in kinetic modeling underway will, in the future, allow improved analysis of the body of data collected in these tests and point to new experiments which will elucidate the problem in this area.

4.1.2 Organic Gas Phase Tests/GC Measurements. The novelty of our experimental approach required that, prior to searching extensively for aerosol formation, we elucidate, if only qualitatively, some of the experimental factors related to the known chemistry of the $NO_2$, olefin, air irradiation. The purpose of these exploratory investigations was to obtain in the time available an understanding of the operational aspects of a gas chromatograph coupled to a fast flow system. Simultaneously, we would determine whether our experimental approach was consistent with the observations of others. The problems of sampling reproducibility and memory effects were considered important from the beginning.

The gas chromatograph and sampling equipment have been described already (Sec. 3.2). Only two aspects of these studies require further discussion: The column choice and conditions and specific sampling conditions. It is our ultimate hope to minimize the number of columns used in the organic analysis; this refers to both the gaseous as well as the condensable ganic materials. To achieve this, consideration was given to selection of a column with a suitable polarity of the liquid phase as well as its ability to withstand injections of water laden samples and reasonably high operating temperatures. Fortunately, Ottenstein and Bartley[42] have considered such factors and it is principally based upon their work that we chose to use a column 1.5 m in length, with 10% SP-1200 / 1% $H_3PO_4$ on 80/100 Chromosorb W AW as the column packing. Although a complete test of this column has not been attempted, our preliminary tests suggest better than satisfactory separation of aldehydes (formaldehyde not tried), monobasic acids, alcohols, alkenes and alkanes, with excellent chances for good separation of organic nitro and nitrate compounds. For the results discussed herein, this column was used at 100°C with a He flow rate of 60 cc/min and flame ionization detection.

The term "sampling conditions" includes conditions used for sample collection to achieve adequate separation and peak shapes as well as conditions necessary to eliminate memory effects.* The best peak shape and separation

*By memory effects we mean the extent to which an analytical measurement depends upon the past history of the sampling components.

were acheived by collection of the gaseous mixture from the sample probe by pumping the mixture through a gas loop cooled to liquid Ar temperature for no more than 4 minutes. The use of liquid Ar eliminated the problems of poor peak shape caused by too large a pressure in the sample loop due to condensation of $O_2$. Prior to sample injection and still with the liquid Ar trap in place, the loop was evacuated and the He stream then passed through the loop. Then flash vaporization was achieved with either a hot water bath or a heat gun. Memory effects were eliminated by careful consideration of the valves with respect to "dead" volumes, virtual leaks, and minimization of O-rings which require even the smallest amount of grease. It should be pointed out that these problems should be given consideration to every region of the flow system, for although the impurities introduce negligible problems in terms of affecting the chemistry (relative to the gases added) their presence may mask the appearance of important products.

The chromatograms produced in Fig. 10 were obtained for the same reactor conditions with regard to residence time (4 sec) $NO_2$ (33 ppm), hexene-1 (2.4 ppm), $N_2$ (750 torr), and sampling procedure (4 min. collection time). The top chromatogram was obtained when $NO_2$, hexene-1, $N_2$ (no $O_2$) flow was sampled by blocking the irradiation from the reactor with an aluminum foil shutter. Peaks C-$F_\Delta$ in Fig. 10 are due to impurities in the hexene-1; their chemical nature was not established as such information was not considered necessary for the initial tests. Peak A is hexene-1 and presumably peak B is hexanal. The origin of the hexanal, a photoproduct, is due to small light leaks around the light shutter. When the same mixture was irradiated two significant changes in the middle chromatogram were apparent; peak B appeared strongly as well as $E_1$, a new peak. When $O_2$ was added to the flow (20%), the lower chromatogram was obtained. Peak B is observed to almost disappear, and the new peaks, $A_1$, $B_2$(?), $B_3$, and $F_1$(?) were observed. Extensive and absolute peak identification using stream splitters, efficient collection, and IR spectroscopy were not considered practical at this time. Tentative identification was achieved by comparing known retention times with authentic samples along with plots of the logarithm of the retention volume vs. number of carbon atoms in a homologous series. In

SC537.10FR

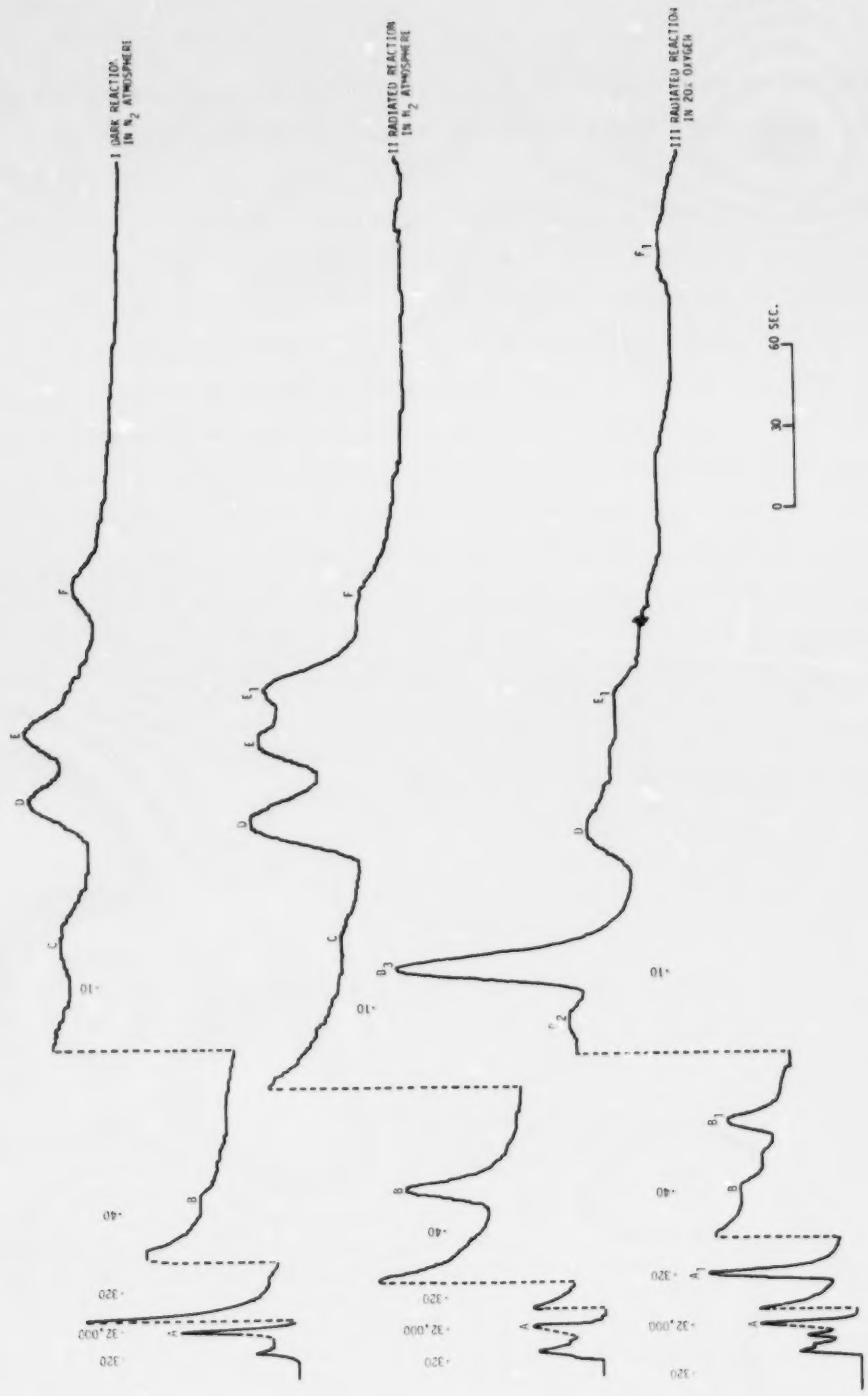


Figure 10 $NO_2$-OLEFIN GAS CHROMATOGRAMS

this manner, peaks $A_1$ and B were assigned pentanal and hexanal respectively. Peaks $B_1$ and $E_1$ were not identified; speculation concerning their identity is given below.

For the purposes of discussing the results of the investigations, a brief digression into the mechanistic details of the reactions $O(^3P)$ atoms with olefins is necessary. Cvetanovic[43] has reviewed the primary reactions of $O(^3P)$ atoms with olefins in $O_2$-free atmospheres as well as discussed the similarities of the products of $O(^3P)$-olefin reaction mixtures containing molecular oxygen with those from the corresponding ozone-olefin reaction. Thus, the irradiation of $NO_2$-air-olefin atmosphere leads to some products that are similar to those formed in (non-irradiated) $O_3$-olefin mixtures (in air). This similarity is accounted for by postulating the following reactions for the case of 1-hexene:

$$O(^3P) + CH_3CH_2CH_2CH_2CH{=}CH_2 \rightarrow CH_3CH_2CH_2CH_2\underset{\cdot}{C}H\text{-}\underset{O\cdot}{C}H_2 \qquad (1)$$

$$CH_3CH_2CH_2CH_2\underset{\cdot}{C}H\text{-}\underset{O\cdot}{C}H_2 \xrightarrow{(M)} \text{epoxide} \qquad (2)$$

$$\rightarrow \text{hexanal} \qquad (3)$$

$$\rightarrow \text{decomposition} \qquad (4)$$

$$+O_2 \rightarrow CH_3CH_2CH_2\underset{\cdot O_2}{C}H_2CH\text{-}\underset{O\cdot}{C}H_2 \qquad (5)$$

$$CH_3CH_2CH_2\underset{\cdot O_2}{C}H_2CH\text{-}\underset{O\cdot}{C}H_2 \rightarrow \text{pentanal} + CH_2O_2(\text{formaldehyde oxide}) \qquad (6)$$

$$\rightarrow \text{formaldehyde} + CH_3CH_2CH_2CH_2CHO_2(\text{pentanal oxide}) \qquad (7)$$

$$\text{formaldehyde oxide } (+O_2) \rightarrow \qquad (8)$$

$$\text{pentanal oxide } (+O_2) \rightarrow \qquad (9)$$

It must be recognized that the above is a condensation and oversimplification of many possible elementary processes about which theoretical arguments may be given. However, such a discussion is not our purpose; rather the reactions given in (1)-(9) are only to provide a basis for discussing our qualitative observations with the results of others. Equations (1)-(4) constitutes the principal reactions which occur in the hexene-1-$NO_2$-$N_2$ mixture, i.e., no $O_2$. As already mentioned, peak B is hexanal while E, although not identified, is approximately where an epoxide would appear on this column (This is based upon a consideration of the McReynolds numbers for SP-1200 column and a carbowax 20 M column. Carbowax 20 M is customarily used for ethers and epoxides.)

Addition of $O_2$ to the reaction mixture introduces a competition between (2) and (5) which under our conditions leads almost exclusively to (5) since hexanal disappears with the concomitant appearance of pentanal. No attempt at formaldehyde detection was made; for the purpose of these experiments its presence was accepted. The absence of hexanal in the $O_2$-containing mixture in these experiments is analogous to the lack of propanal formation in the corresponding propene, $NO_x$, air irradiation, carried out by Altshuller et al.,[44] and to the very small amount (~ 1/30 of propanal) of n-butyraldehyde observed in the sunlight irradiation of $NO_x$-air-butene mixtures by Ellis.[45]

No attempt at the identification of peaks $B_1$ and $B_3$ was made. Based upon polarity arguments of the SP 1200 column packing, they may be postulated to be some organic nitrate. The conditions of these experiments would appear to be particularly conducive for peroxyvaleralylnitrate, pentylnitrate, and peroxypentylnitrate to mention only three. Nevertheless, further speculation concerning the nature of these peaks and therefore the reactions leading them is not warranted without some evidence.

## 4.2 Aerosol Experiments

The aerosol experiments will now be discussed in two parts. First section 4.2.1 will outline some Science Center-funded ozone-olefin aerosol production experiments. These ozone-olefin experiments are discussed at greater length in Appendix B. Then the flow reactor experiments will be detailed in section 4.2.2.

### 4.2.1 Ozone-Olefin Aerosols

As detailed in Appendix B, we have employed a simpler, non-"wall free," reactor to study aerosol production in ozone-olefin reactions. These experiments provided a variety of information, of use in the flow reactor experiments, relating to concentrations and residence times required for aerosol production, and relating to sampling and chemical analysis of aerosols.

The ozone-olefin experiments have shown that a few ppm of reactants and 20 to 40 seconds of residence time are required for production of light scattering aerosols. While these conditions are possible within the flow reactor, they were not achieved in the experiments described below. This was a major input to the decision to move ahead to the addition of other components ($SO_2$ and $H_2O$) to the reaction mixture in the flow reactor experiments.

The aerosols produced in the ozone-olefin experiments were also used to test the efficiency of collection of the sampling probes used with the flow reactor and to test the IR and GC-MS methods of analysis for collected aerosols. These chemical analysis methods proved very useful in generating information about the aerosols produced and are discussed in detail in Section B.3.

### 4.2.2 Flow Reactor Aerosol Experiments

As a program for determining the conditions for aerosol production in the flow reactor, a series of preliminary tests were undertaken. Several sets of conditions in the $NO_2$-olefin-dry air system were tried including cases with a few ppm to hundreds of ppm of olefin and a few ppm to a hundred ppm of $NO_2$. Table 6 shows a summary of the conditions under which no aerosol was produced. After aerosols were detected in the $NO_2$-olefin-$SO_2$-$H_2O$-air system, no further tests were made on the $NO_2$, olefin, dry air system. It was decided to test the sampling and chemical analysis techniques on these aerosols produced by the 1-hexene and $NO_2$ system with $SO_2$ and $H_2O$ present.

In the $NO_2$-olefin-$SO_2$-$H_2O$-air system the necessity of each component, for aerosol production, was checked. Figure 11 shows the strip chart response

Table 6

Conditions Under Which No Aerosols Were Produced in the Reactor

| $[NO_2]$ ppm | [1-Hexene] ppm | $[O_2]$ % | Residence Time sec. |
|---|---|---|---|
| 6 | 50 | 21 | 10 |
| 8.7 | ~ 678* | 20 | 5 |
| 10 | 4.6 | 10 | 12 |
| 10.5 | 50 | 21 | 10 |
| 13 | 50 | 21 | 10 |
| 13 | ~ 678* | 20 | 5 |
| 17 | 4.4 | 10 | 12 |
| 17 | 50 | 21 | 10 |
| 17.7 | 8.7 | 10 | 12 |
| 20 | 4.4 | 20 | 10 |
| 20 | 10.8 | 20 | 10 |
| 20 | 26 | 20 | 10 |
| 20 | 50 | 21 | 10 |
| 20 | 61 | 20 | 10 |
| 20 | 78.1 | 20 | 10 |
| 20 | 114.1 | 20 | 10 |
| 22 | ~ 678* | 20 | 5 |
| 30 | 50 | 21 | 10 |
| 51 | ~ 678* | 20 | 5 |
| 54 | 50 | 21 | 10 |
| 70.6 | ~ 678* | 20 | 5 |
| 104 | ~ 678* | 20 | 5 |
| 189 | 50 | 21 | 10 |
| 197 | 50 | 21 | 10 |

*Rotameter by-passed

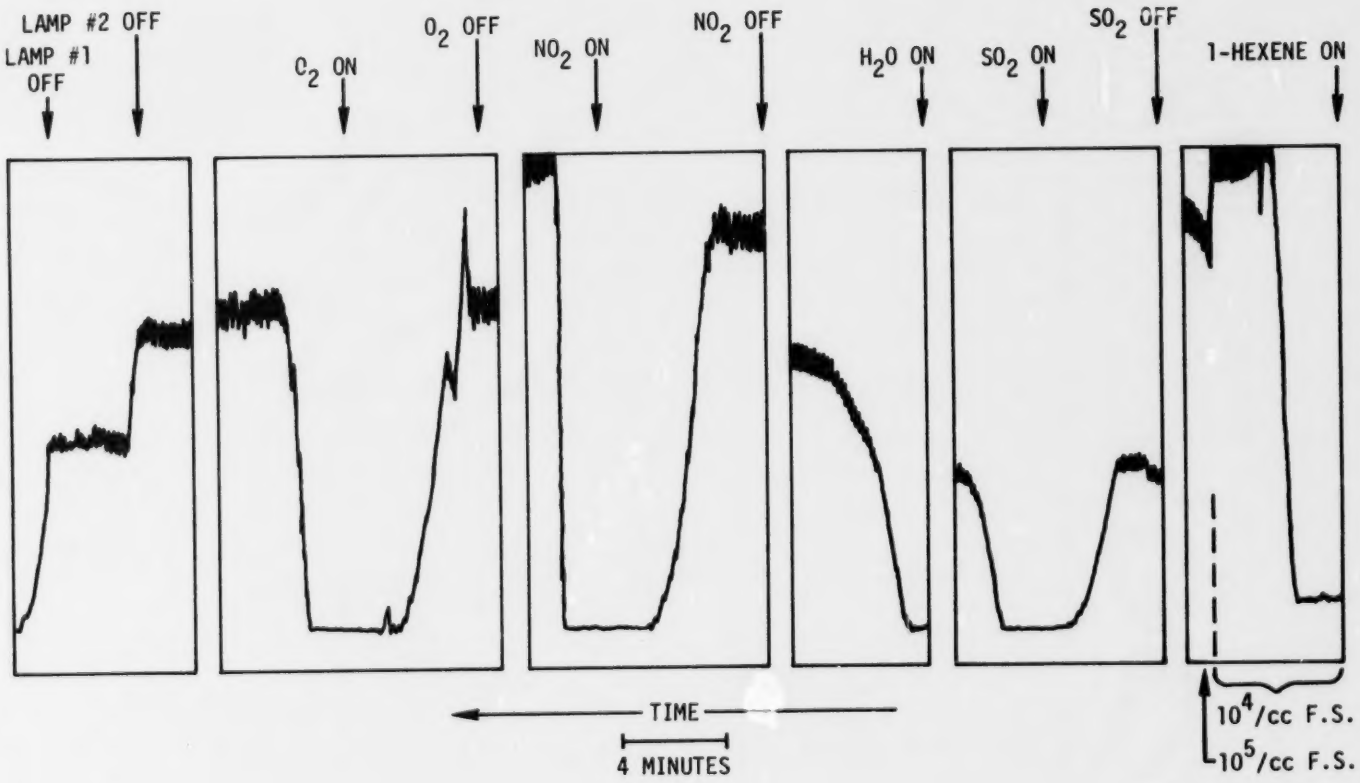


FIG. 11 CNC STRIP CHART RECORDING: $10^7$ NUCLEI/CC FULL SCALE
(TWO MERCURY VAPOR UV LAMPS)

to the output from the condensation nuclei counter at different points in time during a reactor experiment. The sharp response of the CNC when each gas is valved off and turned on again implies a strong dependence of the aerosol production rate as a function of the concentration of each individual gas component. Finally, the drop in aerosol count as the UV source was halved and then turned off implies that the aerosols produced are photochemical in nature. Reactor conditions for various experiments are shown in Table 7.

The aerosol generated were predominately in the submicron size range. The General Electric portable condensation counter indicated counts of $10^7$ nuclei per cubic centimeter (maximum reading) or greater. The Royco 225 optical counter did not indicate significant particle concentration above the noise level of a few particles per cubic centimeter. Data from weighed filter samples (0.1 μ Nuclepore) indicated mass concentrations of about 80 μg per cubic meter in the reactor under conditions shown in Table 7 for filter collected samples.

### 4.3 Chemical Analysis of the Aerosol Samples

Since the aerosols were formed in the presence of $SO_2$ and water vapor, we first sought sulfate in the aerosol samples. In addition, as previously planned, both nitrate and organic analyses were carried out. Since a large amount of sulfate was found in the samples, it was expected that the organic component would be small, so only a total organic measurement was made. The sulfate analyses were satisfactory, but some problems arose with the analysis for nitrate. Only an upper limit on organic content was determined.

#### 4.3.1 Sulfate Analysis

Typically, it was found that for a 16 hour reactor run, about 50 to 150 micrograms of aerosol were collected, and it was anticipated that the sulfate content would be in the high nanogram to low microgram range. An analytical method was therefore needed which has the sensitivity to determine this amount of sulfate. The classical method for determination of small amounts of sulfate is the turbidimetric method. There was some

Table 7

CONDITIONS USED FOR AEROSOL PRODUCTION FROM $SO_2$, $H_2O$, $NO_2$, & AN OLEFIN IN AIR

| | Nuclei Production (1) | Nuclei Production (2) | Filter Samples for Chemical Analysis |
|---|---|---|---|
| $[O_2]$ | 18% | 18% | 18% |
| $[H_2O]$ Relative Humidity | 50% | 50% | 44% |
| [1-Butene] | - | 15 ppm | - |
| [1-Hexene] | 18 ppm | - | 75 ppm |
| $[NO_2]$ | 20 ppm | 20 ppm | 47 ppm |
| $[SO_2]$ | 8 ppm | 8 ppm | 7.7 ppm |
| Residence Time (average) | 4 sec | 4 sec | 4 sec |

question as to whether this method would have the sensitivity and accuracy required. Another method which has been proposed by Scarengelli[46] involves volatilizing sulfuric acid, reducing it to $SO_2$ and measuring the $SO_2$ with a flame photometric detector. This method is stated to have a sensitivity in the nanogram range, but the method was not found to be workable as described. It has been learned recently that the method can be modified and simplified to give adequate results.[47]

Previous experience with the method of Fritz[48] suggested that this method might be modified to give the sensitivity, analytical simplicity and accuracy desired, particularly if the amount of sulfate present was 5 µg or above. This method involves the titration of sulfate with barium perchlorate in 80% isopropanol solvent using thorin [2(2-hydroxy, 3,6-disulfo-1-naphthyl azo) benzene arsonic acid] as the indicator. To decrease the detection limit and improve the titration, the final solution volume was reduced to near 5 ml, the end point was obtained by comparison against suitable standards with application of appropriate indicator blanks, and a micro buret was employed which allowed adding increments of $5\times10^{-6}$ mill-equivalents of barium ion (equivalent to 0.5 µg sulfate). The smallest amount of sulfate which can be determined by this technique is approximately 4 µg, with an uncertainty of about ± 1.5 µg. If a spectrophotometric titration is used where the absorption peak of the barium thorin complex at 5500Å is employed for end point detection, the detection limit can be decreased to about 2 µg with an uncertainty of ± 0.5 µg using a 3 cm path length, and probably lower with a longer path length cell.

The presence of cations other than hydrogen ion can interfere in this titration. The interference is less with the spectrophotometric titration since some ions (e.g. $Na^+$) only react with some of the indicators to give an interfering color. This can be compensated for spectrophotometrically. In the aerosol samples, no cations other than hydrogen ion would be expected except as impurities and the greatest source of these would be the filters employed. Consequently, the papers were washed thoroughly before use. Anions also can cause some error in this titration because of coprecipitation. From the work of Fritz et al.,[48] the presence of a 6 fold excess of nitrate

(an anticipated aerosol component) over sulfate will cause an error of about 5% in the titration. No other interference appears likely. It is, therefore, expected that the accuracy of the titration is well within 10%.

While complete recovery of known amounts of sulfuric acid was possible when added directly to the solution, recovery was very poor when the acid was placed on glass fiber filters (Gelman A) and extracted off the paper. We found recoveries which varied from almost 0 to 80% depending on the paper lot and level of sulfate. This is in agreement with the literature[46,49] and has been attributed to the presence of "alkaline sites" on the paper. We were not successful in finding a simple acid washing procedure to neutralize these sites effectively, although we did not try some of the more elaborate techniques which have been proposed.[46,49] In order to avoid this problem with glass fiber filter papers, we employed Nuclepore papers as the filter media. Sulfate recovery was quantitative using these papers and very little blank or cation impurities were found. The papers, however, were still washed before use as a precautionary measure. In the procedure the filters were extracted with 3-1 1/2 ml portions of 80% isopropanol solution to remove the sulfate for subsequent determination.

Several preliminary analyses of 16 hour reactor runs showed quantities of sulfate in the 20 to 30 μg range. Since this was considerably more sulfate than required for analysis, the time of the run was reduced in the interest of time economy. Two 3 hour reactor runs were made under the following conditions. Concentrations of oxygen, 1-hexene, nitrogen dioxide, and sulfur dioxide were 18%, 75 ppm, 47 ppm, and 7.7 ppm, respectively, with 44% relative humidity and a residence time of about 4 seconds. In the first run, the aerosol was found to contain 18% sulfate and in the second it contained 16%. A run made under the same conditions, but with the UV light of the reactor off, showed no sulfate on the filter paper. These limited data show the feasibility of making detailed correlations between reactor conditions and aerosol composition.

4.3.2 Nitrate Analysis. Since the participation of nitrate in aerosol formation is an important aspect of this program, various methods were considered for the analysis of microgram aerosol samples for small amounts of nitrate. The standard method using 2,4 xylenol[50] appeared to be rather complicated and to lack the sensitivity required. The use of chromotropic acid[51] and 1-amino pyrene[52] are described as having sensitivities which were expected to be suitable (~ 1 μg $NO_3^-$) but our evaluation of these methods showed them to be highly irreproducible and very dependent on small details of the procedure. In using chromotropic acid the absorbance of reagent peaks without nitrate was found to be excessive.

The wide experience of Science Center personnel with polarographic and pulse polarographic[53] techniques allowed evaluation of various modified polarographic techniques for analysis of microgram quantities of nitrate. It was found that the method of Kolthoff, Harris and Matsuyama[54] which involves the catalytic reduction of nitrate during the reduction of uranyl ion could give a sensitivity to nitrate of about 2 μg $NO_3$ if a derivative pulse polarographic procedure was used.[53] The procedure devised was exceedingly simple and involves extraction of sample from the paper, placing it in a 10 ml volumetric flask, adding 2 ml of uranyl ion "activator" and taking the derivative pulse polarogram. The activator solution pulse polarographic peak height is subtracted from the peak height of the sample polarogram and this difference is related to the concentration of nitrate through a previously derived linear calibration plot. Very few interferences exist in this method. Concentrations of sulfate 50 times that of nitrate have no effect but very large amounts can decrease the nitrate current somewhat. (See Kolthoff and Lingane[54] for further discussion of the classical method.) The method is sensitive, accurate and precise and is much simpler and more rapid than the colorimetric methods if a pulse polarograph is available.

The polarographic technique does not directly distinguish between nitrate and nitrite. In other words both nitrate and nitrite are catalytically reduced by uranyl ion. However, since different numbers of electrons are involved in the two reductions, the amount of nitrate and nitrite separately can be obtained by taking the polarogram before and after nitrite oxidation.

The ratio of nitrate to nitrite in our samples will be determined in the future.

Preliminary analysis of filter papers from reactor runs showed rather large amounts of nitrate on the filter. However, when two filters were placed in the probe back to back, a considerable amount of nitrate was found on the back filter. Nitrate was also found with the UV light off and even with no $NO_2$ in the gas mixture. Quantitative determinations of nitrate showed that a 6 hour run without $NO_2$ give 18 µg $NO_3$ on the filter, a 6 hour run with only $N_2$ gas flowing through the reactor gave 4 µg of $NO_3$ on the filter and a filter paper put through all the handling procedures of the above samples showed about 2 µg of nitrate. The uncertainty of all these measurements was ± 1 µg.

The explanation for this behavior is not apparent, but should be readily explainable with a few additional experiments. There are three possibilities which can be advanced. Perhaps most likely is that the walls of the probe used to collect the sample on the filter papers (see reactor design) is contaminated from previous experiments and the water vapor in the gas mixture is desorbing or otherwise removing nitric acid. The nitric acid is then adsorbed on the filter paper surface. The fact that nitrate is generally found on the walls of smog chambers lends some credence to such a hypothesis. The second hypothesis involves the possibility of $HNO_3$ or $NO_2$ (or other nitrate former) contamination in one of the gases used in the gas mixture. The third possibility, that of contamination from the reactor walls, seems less likely since calculations indicate that material from the reactor walls should not be captured by the probe because of the laminar flow maintained.

### 4.3.3 Total Organic Analysis

The experimental procedure in the effort to detect and measure the total organics or the total hydrocarbons was to compare filter samples collected from the reactor with and without UV irradiation, the non-irradiated sample being the background signal. However, we still have the problem of differentiating the "aerosol signal" from the organic gas phase reaction products adsorbed on the filter substrate. Therefore, it was decided to collect

aerosol samples using tandem filters. The front filter sample would have both the adsorbed gas phase reaction products and the collected aerosol. The second filter should have only the gas phase products if we assume the front filter is efficient in removing particulates from the gas stream.

The hydrocarbon detector used for the analysis was the hydrogen flame ionization detector also used with the Loenco Model 70 gas chromatograph. A filter sample was placed in a helium atmosphere inside a hermetically sealed container which was then heated to 150°C for thirty minutes. Material which is volatile at 150°C was driven off the filter paper and flushed into the flame ionization detector by the helium carrier gas. A capillary tube served as a flow restriction to prevent the volatilized gases from blowing out the hydrogen flame but otherwise no column was used. The whole length of the sample path from the sealable container, through the valve, to the detector was heated to prevent sample recondensation.

Although the FID has a satisfactory sensitivity at low sample concentrations, in the ppb range, the overall measurement sensitivity is significantly impaired by large background level masking the sample signal. As the hermetically sealed container is heated to high temperatures, any residual contaminants from the stainless steel fittings, valves or Viton O-rings begins to be liberated and interfere with the analysis. Adsorbed or absorbed contaminants also are liberated from the glass fiber filters themselves.

A known weight of hexadecane (9 μgm) was placed on a filter and carried through the extraction procedure. Relative to this calibration the organic content of the aerosol samples is equal to or less than 1.5%.

## 4.4 Discussion of Aerosol Results

We have shown that aerosols can be formed, under at least one set of conditions in the flow reactor, which has some connection with actual atmospheric aerosols. In addition we have tried other systems and not observed aerosols under conditions in the flow reactor. The sulfate aerosol formation which we have observed has already been studied extensively and is not the most interesting case for study in the flow reactor. However, there are interesting aspects of it relating both to the gas phase

oxidation of $SO_2$ and the growth of the nuclei which may be elucidated in the flow reactor. The data from the ozone-olefin experiments indicate that a longer residence time will probably be required for organic aerosol production in the $NO_x$-olefin-dry air case. As we have seen in Section 2 the "wall free" criteria can be achieved for longer residence times by modification of the reactor.

The data obtained for the formation of the sulfate aerosols are consistent with the following mechanism:

$$SO_2 + RO_2\cdot + H_2O \xrightarrow{J_c} H_2SO_4 + RO\cdot$$

$$n^*H_2SO_4 \xrightarrow{J^*} (n^*H_2SO_4)_{cluster}$$

$$A_{n,m} + H_2SO_4 \underset{J_{1-}}{\overset{J_{1+}}{\rightleftharpoons}} A_{n+1,m}$$

$$A_{n,m} + H_2O \underset{J_{2-}}{\overset{J_{2+}}{\rightleftharpoons}} A_{n,m+1}$$

Where $J_c$ is the rate of formation of condensable material ($H_2SO_4$), n* is the critical number of molecules for a growing nuclei, J* is the rate of formation of such nuclei and $J_{1+}$, $J_{1-}$, $J_{2+}$, $J_{2-}$ are rates of gain or loss of one molecule of either $H_2SO_4$ or $H_2O$ from a particle $A_{n,m}$ containing n molecules of $H_2SO_4$ and m molecules of $H_2O$. Although there are potentially an infinite number of species and, even for our cases, a very large number, mathematical techniques are available to analyze such systems of reactions. In addition thermodynamic data can be employed to estimate $J_{1\pm}$ and $J_{2\pm}$ as well as $J_*$. The analysis of this mechanism in the flow reactor should prove useful as a preliminary to unfolding the more complex mechanism expected for the organic aerosols. The experiments carried out so far for filter

collection of the sulfate aerosol have been carried out at high concentrations to increase the amount of material collected (see Table 7) in order to validate the chemical analysis techniques. These must be repeated at lower concentrations to check the variation with concentration.

## 5. Summary and Recommendations

We will now summarize the material presented in this report as it applies to three tasks set forth in the APRAC contract. Conclusions from the data and recommendations for further work will be included.

### 5.1 Aerosol Production

In the flow reactor with a 4 second residence time and 10-20 ppm each of $NO_2$, 1-hexene, $SO_2$, $H_2O$ in air aerosols were formed. These were detected by a condensation nuclei counter and collected on various filters. Aerosols were sought but not produced under a variety of conditions in the system including $NO_2$, 1-hexene, and dry air. These experiments however were not exhaustive.

For the case of $SO_2$ present, it was shown that all components including $O_2$ and light were required for nuclei production. The aerosols were collected with, among others, Nuclepore filters which had 0.1 μ pores. However they were not detected by an optical particle counter suggesting that they were probably much smaller than 0.1 μ and were collected by diffusion in the pores of the filter.

In a separate, Science Center funded, series of experiments, aerosols were produced by ozone-olefin reactions in a simpler reactor.

### 5.2 Chemical Analysis

Both aerosols produced in the flow reactor and in the ozone-olefin experiments were chemically analyzed. Those formed in the presence of $SO_2$ were found to contain about 20% $SO_4^=$ and negligible (less than 2 μgms in 50-100 μgm sample) organic material; the analysis for $NO_3^-$ was not definitive. While $NO_3^-$ was found in the samples, possible paths for contamination were determined. The presence of $NO_3^-$ in the filter sample does not mean it was present in the aerosol but that it may have condensed on the filter or the filter holder directly from the gas phase or may even be left on the filter holder from previous runs.

Aerosol from the ozone-olefin experiment was used to evaluate the infrared and GC-MS methods. This aerosol was found to be a highly-oxygenated oxidizing compound or compounds. The IR spectrum had strong similarities

to aerosols formed in smog chambers and collected in the atmosphere. The principal identified products in the GC-MS analysis appeared most likely to be decomposition products. In addition iodimetry and polarography were used to study the oxidative nature of the aerosol samples.

## 5.3 Data Analysis and Feasibility

The production and collection of aerosol in the irradiated $NO_2$, $SO_2$, $H_2O$, hydrocarbon, and air system has shown that it is feasible to study aerosol production and composition with a fast flow reactor. This was carried out over a large range of conditions (Table 7) which should allow for extrapolation to atmospheric levels. The data we have gathered are consistent with a simple mechanism, presented in section 4.4, although it is as yet insufficient to determine any details of such a mechanism.

The preliminary work on the $NO_x$, olefin, and dry air system while it has not produced aerosols has shown that aerosol production should be possible in a fast flow reactor. The residence time however as shown by the ozone-olefin reactions may have to be somewhat longer. In addition very complete knowledge of the inorganic chemistry will be required to achieve the proper conditions for aerosols in the reactor. Progress has been made in modeling the gas phase kinetics necessary for understanding this problem completely.

## 5.4 Recommendations

Considering the accomplishments already achieved under this program, we recommend further work on the $NO_2$, olefin, and dry air system. This should begin with a systematic study of the gas phase reactions in the reactor to check the possibility of generating conditions under which aerosols can be produced. Kinetic modeling should play an important role in this part of the program. It is possible that modification might have to be made in the reactor system to achieve the stated goal. The range of possibility for this, within the "wall free" design criteria, were discussed in Section 3. Further development of aerosol models, such as that of Section 4.4, for the organic aerosol case should be undertaken as part of this program.

## APPENDIX A. Modeling, Mechanism and Simulation

Of central importance to understanding experiments undertaken in the flow reactor and applying the results to real atmospheric problems is our ability to unfold the mechanism of aerosol formation and successfully model it together with the gas phase kinetics. In this appendix we first discuss an example of scaling of a complex reaction and then go on to details of improved concepts in modeling both aerosol formation and gas phase kinetics.

### A.1 Scaling of Reactions

As discussed in Section 3, in order to have an atmosphere simulation reactor in which the walls are unimportant, it is necessary to go to short residence times compared with normal atmospheric time scales. Two types of scaling are possible. In the first, the concentration of reactants and the light flux may be changed so that the entire part of the reaction of interest takes place during the residence time in the reactor, thus achieving an overall time scaling. The second is a differential approach wherein, by changing reactant concentrations to approximate those in the atmosphere, and possibly by adding products, one may examine a short period of time during the overall reaction. To accomplish both of these alternate approaches for certain gas phase mixtures and assumed mechanisms, simplifications and assumptions have to be considered. These are described, and an extension of these ideas is made to aerosol formation to show how the data taken from scaled reactions may be interpreted.

To illustrate the basis of the gas phase scaling, the Friedlander-Seinfeld model of the kinetics of photochemical smog is used.[22] While this model includes only a few reactions, and is obviously not a complete model of photochemical smog, it is very useful for the present purpose. It concerns itself specifically with the $NO_x$-hydrocarbon system which will be central in our studies. The reactions considered may not be complete, but they represent a plausible mechanism that is general enough to include the possibility of some variation. The gas phase reactions included are:

$$NO_2 + h\nu \rightarrow NO + O$$

$$O + O_2 + M \rightarrow O_3 + M$$

$$O_3 + NO \rightarrow NO_2 + O_2$$

$$O + RH \rightarrow R\cdot + \text{products}$$

$$O_3 + RH \rightarrow \text{Products}$$

$$NO + R\cdot \rightarrow NO_2 + R\cdot$$

$$NO_2 + R\cdot \rightarrow \text{Products}$$

where RH is some hydrocarbon, R· is a generalized free radical (which includes R·, RO·, $RO_2$·, etc.), and M is a third body.

By a series of approximations Friedlander and Seinfeld reduced the kinetic equations for this system to:

$$\frac{d[NO_2]}{dt} = [NO_2][RH]\{\alpha[NO]-\lambda[NO_2]\} \qquad (A.1)$$

$$\frac{d[NO]}{dt} = -\alpha[NO_2][NO][RH]$$

$$\frac{d[RH]}{dt} = -[NO][RH]\{\theta+\mu/[NO]\}$$

$$[O] = \gamma[NO_2]$$

$$[O_3] = \beta\frac{[NO_2]}{[NO]}$$

$$[R\cdot] = k_4'[RH\ [O]$$

where $\alpha$, $\beta$, $\gamma$, $\lambda$, $\mu$, $\theta$, and $k_4'$ represent various groups of rate constants of the elementary reactions; $\alpha$, $\beta$, and $\gamma$ also depend linearly upon the light intensity.

An important observation about the results of the Friedlander-Seinfeld model is that the O, $O_3$, and R· concentrations were arrived at by use of steady state approximations. It is assumed that these concentrations adjust to the values given in a time short compared with other characteristic times in the reactions. For example in the above model the oxygen atom concentration reaches $\gamma[NO_2]$ in microseconds when the time scale for significant changes in reactants is minutes. An important advantage of this model is that a partially analytical solution of the system of rate equations has been found.[55] In this solution the $NO_2$ and RH concentrations are expressed as functions of the NO concentration and time is expressed as an integral of a function of the NO concentration. This integral may be easily solved numerically and has analytical solutions for various limiting cases.

We can use the model to demonstrate how reaction times may be scaled in a simulation experiment. The integral for time in the solution described above may be written in the form,

$$t = \tau\nu \int_{[NO]/[NO]_o}^{1} f(x,\nu,\delta,\kappa)dx$$

where

$$\nu \equiv [NO_2]_o/[NO]_o$$

$$\tau \equiv \frac{1}{\alpha[NO_2]_o[RH]_o}$$

$\delta$, $\kappa$ are parameters depending upon the initial concentrations and the rate constants, and $\alpha$ is a rate constant grouping which is linearly proportional to light intensity. The parameters $\delta$ and $\kappa$ are important only for long times. We may define a dimensionless time $\tilde{t} = t/\tau$. Now the actual reaction time t in the system may be scaled by the parameter $\tau$, since $\tilde{t}$ will be approximately constant if $\nu$ is kept constant. Numerical tests have shown that $\kappa$ and $\delta$ are completely negligible for times such that the reactions have gone one half way to completion (beyond the peak in $NO_2$ concentration).

Suppose a concentration scale factor m is introduced. Scaling is achieved by multiplying each of the factors in $\tau$ by m. Then $\tau$ is changed by a factor of $m^3$, or for m = 10 the reactions are accelerated by 1000.

If the mechanism in the Friedlander-Seinfeld model included all possible reactions in the $O_2$-$NO_x$-hydrocarbon photolysis, then our work would be done any any value of m would be acceptable. However many possible reactions are missing and some of these will be higher order in the concentrations we are varying than the ones which have been included. Thus there are limits on the value which m may take on and for some conditions it might be better for us to have different multipliers for the different factors in $\tau$. Assuming that each of the three factors in $\tau$ is multiplied by m, we must estimate the initial changes in concentration of the various reactants. From equations (A-1) we see that [O], [$O_3$], and [R•] will be multiplied by $m^2$, m and $m^3$ respectively. Thus the most important species to consider first are R•; the only removal mechanism included in the model is the reaction of R• with $NO_2$; however, radical-radical recombination may also become important. The R•+$NO_2$ reaction will increase in rate by a factor of $m^4$ but radical-radical recombination will increase by $m^6$. Unfortunately, rate constants for these reactions are not generally known, but it is not unreasonable to set them equal. Using the numerical estimates from the paper of Friedlander and Seinfeld[22] and an estimate of 10 $ppm^{-1}min^{-1}$ for the recombination rate, we get a ratio

$$\frac{[R\cdot]}{[NO_2]} = 4 \times 10^{-4} .$$

So with respect to this reaction with an m of 10, which multiplies this ratio by 100, the neglecting of radical-radical recombination will still be a good approximation, but as m get larger than 10 the neglected reaction rapidly becomes comparable to the reaction in the model.

Another similar consideration is the comparison of other oxygen atom recombination rates which increase by a factor of $m^4$ with the formation of $O_3$ from O+$O_2$ which only increases by a factor of $m^2$. In this case, however,

several reactions of O atoms with oxides of nitrogen will scale as $m^3$ and have been considered. The most important of these is $O+NO_2 \rightarrow NO+O_2$, which with m = 10 has 4% of the rate of the reaction with $O_2$. The ozone reactions as well as reactions between oxides of nitrogen do not appear to create any problem since all the excluded reactions scale with the same low powers of m as the included reactions. This means that $m^3$ of the order of a few thousand is possible which will reduce reactions taking 15 minutes to one hour at the 1-2 ppm level to a few seconds at higher concentrations. It is important to observe that changing the times by such large factors does not just multiply all the concentrations as a function of time by a fixed amount. Rather, the ultimate products remain the same, but possibly in quite different relative amounts. The set of important elementary reactions, however, remains the same and once verified may be used to extrapolate the results back to the concentration levels desired.

Another method of "scaling" is to make a differential measurement. That is, reactions may be carried out over short times in the flow reactor in a sequence such that their summation generates concentration - time curves equivalent to processes over a much longer time interval. This method has the drawback that it requires not only introducing starting reactants but also all intermediates and products that are expected to react further. Although this appears to be an almost impossible task, if we look back at the Friedlander-Seinfeld model we employed for overall scaling, we can make an interesting and very useful observation. The model reproduces the important features of the photochemistry by employing steady-state approximations for all intermediate species including products such as ozone which also takes part in further reactions. If the dominant intermediate reactions can be approximated well by steady state assumptions, then all that is required is to start the reactants in varying concentrations, and the intermediates will quickly come to their appropriate steady state values in a time short compared to the period of time being studied. If an intermediate does not come to equilibrium in a time short compared to the residence time, then it must be added to the reaction mixture. This may be true for ozone under some of the conditions used in this study. One may then step through

a reaction system differentially by either predicting concentrations as a function of time and checking the consistency of differential rates measured or by proceeding with each step based upon the results of the previous step.

In the experiments described in this report a combination of the two methods was used. The reactants are set ahead to the point where there is no NO present and the remaining concentrations are increased to speed up the resultant reactions. A potential problem with this procedure is that the scaling described above works best in the early stages of the smog reactions when NO is still present. In addition, aerosols are not included and do not fit well into such a simple model.

A2. Extrapolation of Laboratory Experiments to Atmospheric Transformations

The modeling of physical processes historically has been a key feature in the development of engineering methods, and it is particularly useful in extrapolating from a model system to a prototype involving fluid dynamics. Model-prototype dynamics also has been useful in studying atmospheric processes involving air motion. The exact duplication of a prototype by a model can be achieved by proper scaling of all relevant parameters required to characterize the behavior of the system. However, many models have usefulness with only partial scaling of key parameters between prototype and model. Examples of simple modeling are discussed in Bridgman's classic book[56] and in Birkhoff's monograph.[57] Atmospheric applications have been reviewed by Hidy.[58]

The modeling of aerosol formation by chemical reactions in the atmosphere should be feasible, provided key dynamic parameters can be identified and scaled such that a simulation can be realized. At this stage a detailed modeling scheme based on knowledge of the kinetics of atmospheric aerosol formation is difficult to project quantitiatively. This is particularly true with the uncertainty as to whether or not atmospheric aerosol growth takes place by formation of condensable precursors solely in the gas phase, followed by irreversible (vapor) diffusion controlled nucleation or deposition on existing particles or by surface catalyzed chemical reactions to form stable products on existing particles. Despite the continuing field

work devoted to clarification of this question, there is little more than speculation on which to base a judgement on alternative mechanisms. However, one can derive a hypothesis on which to base a first approach to modeling with the following assumptions:

1. Condensed material in the atmosphere is essentially in thermodynamic equilibrium with the gas phase.

2. The production of aerosol precursors by photochemical (or other chemical) reactions is the rate controlling step in atmospheric aerosol formation.

3. The existing aerosol in the atmosphere can be characterized by averaged properties of volume fraction, $\langle V \rangle$, total surface concentration, $\langle \sigma \rangle$, a surface chemical potential (per unit gas volume) $\mu_s$, and a bulk chemical potential $\mu_i$.

We note that essentially three kinetic processes must be considered:

precursor formation

$$\frac{dX_1}{dt} = R_1(X_1 \text{ --- } X_n, P)$$

$$\frac{dX_n}{dt} = R_n(X_1 \text{ --- } X_n, P)$$

$$\frac{dP}{dt} = R_p(X_1 \text{ --- } X_n, P)$$

where $X_1$ --- $X_n$ are reactants and intermediates and P is the aerosol precursor.

nucleation

$$J \sim \exp\left(\frac{\gamma^3}{T^3 \ell n^2 S}\right)$$

where J is the number of particles formed per cc per second and $\gamma$ is the surface free energy of the condensing species, which depends on the temperature T, and the product P, and S is the supersaturation ration $p/p_\infty$, where $p_\infty$ is

the equilibrium vapor pressure of species P, $p_\infty$ is a function of temperature only.

vapor diffusion limited deposition $\Phi \sim v^x(S-1)$

where x is an exponential ranging from unity to two-thirds.

Suppose the aerosol formation process is characterized in terms of the distribution function $n(v,\mu_j,t)$, where $n(v,\mu_j,t)dvdt\,\delta\mu_j$ is the number of particles in a volume range between v and v+dv, in a time interval t and t+dt, and with a chemical potential difference from a standard $\delta\mu_j$ (j = s or i).

Then formally, the aerosol modeling hypothesis in simplest form is expressed in terms of ratios in a functional form:

$$\frac{n_p}{n_m} = \psi_1\left(\frac{\langle\mu_{ip}\rangle}{\langle\mu_{im}\rangle}, \frac{\langle\mu_{sp}\rangle}{\langle\mu_{sm}\rangle}, \frac{\langle v_p\rangle}{\langle v_m\rangle}, \frac{\langle\sigma_p\rangle}{\langle\sigma_m\rangle}, \frac{T_p}{T_m}, \frac{P_p}{P_m}, \frac{\dot{P}_p}{\dot{P}_m}\right),$$

where p is the prototype property and m is the model property. The first model approach is to initially simplify further by assuming that

$$\frac{\langle u_p\rangle}{\langle u_m\rangle} \approx \frac{\langle\sigma_p\rangle}{\langle\sigma_m\rangle} \approx 1, \frac{T_p}{T_m} \approx 1,$$

$$\frac{\langle\mu_{ip}\rangle}{\langle\mu_{im}\rangle} \approx 1, \text{ and } \frac{\langle\mu_{sp}\rangle}{\langle\mu_{sm}\rangle} \approx 1$$

can be achieved, and

$$\left(\frac{n_p}{n_m} \approx \psi_2\ \frac{P_p}{P_m}, \frac{\dot{P}_p}{\dot{P}_m}\right)$$

Thus, as an initial modeling criterion, the problem is reduced to considering a scaling of aerosol formation reactions in terms of aerosol precursor ratios and the ratios of rate of formation of such material. As initially proposed, the key to such a modeling strategy now relies heavily on the ability to

quantify the gas phase chemical kinetics sufficiently well to look for scaling ratios between model and prototype.

A.3 Mathematical Modeling of Gas Phase Kinetics

We are now using a variety of mathematical techniques to incorporate the pertinent rate data into kinetic models for analysis of planned experiments and data. These range from simple analytical models to complete numerical solution of the differential equations of the system of equations. The more sophisticated numerically oriented methods allow much flexibility in the inclusion of individual reactions. Simple numerical analysis is achieved by conventional techniques using pseudo steady state approximations and obtaining those integrals which are available analytically, followed by numerical solution. The numerical solutions are carried out on an interactive terminal to an IBM 360 computer in APL ("A Programming Language"). Typical output from this system is shown in Figures 12 and 13. The calculations shown were used in understanding the $NO_x$ in air photolysis. The output generated could be saved and manipulated in real time. A typical result of such a manipulation is shown in Figure 14 and represents a cross-section of output from many graphs of the form of Figure 13. This system of analysis is limited in the number variables, the speed of calculation, and accuracy of approximations.

We are now nearing completion of a general reaction kinetics program for the CDC 6600 computer. This system employs advanced solution techniques[59] for stiff differential equations. Its most important feature however is the addition of reaction by insertion of single data cards and the ability to analyze relative rates at any point during the calculation. Many additional features are being considered for this program but the most important factor is that this modeling effort can be tied closely to the experimental program. Both proposed mechanisms and experimental results will be analyzed quickly and efficiently.

We have not employed this system yet to completely analyze a reactor experiment but some test output is now presented to demonstrate its capability. Figure 15 shows the input of a set of reactions as it appears on the computer

10/26/72

6 REACTIONS INCLUDING O +NO2 → NO + O2
O +NO2 → NO3
O3+NO2 → NO3 + O2

K1= 0.0056

| TIME(SECS) | [NO2] | [O3] | [NO] |
|---|---|---|---|
| 0 | 10 | 0 | 0 |
| 1 | 9.942074665 | 0.05273074587 | 0.05666404282 |
| 2 | 9.886604424 | 0.1015436648 | 0.109366355 |
| 3 | 9.835802371 | 0.1443868715 | 0.1560580706 |
| 4 | 9.790899868 | 0.1802295949 | 0.1957127144 |
| 5 | 9.752197277 | 0.2089822548 | 0.2282455158 |
| 6 | 9.71931611 | 0.2312219363 | 0.2542382649 |
| 7 | 9.691499308 | 0.2478790328 | 0.2746255665 |
| 8 | 9.667858021 | 0.2599855087 | 0.2904429287 |
| 9 | 9.647530816 | 0.2685162695 | 0.3026681102 |
| 10 | 9.629764456 | 0.2743118765 | 0.3121438996 |
| 11 | 9.613940831 | 0.2780561825 | 0.3195558516 |
| 12 | 9.599573459 | 0.2802843626 | 0.3254404231 |
| 13 | 9.586290154 | 0.2814042202 | 0.330206375 |
| 14 | 9.57381169 | 0.2817207791 | 0.3341594432 |
| 15 | 9.561931415 | 0.2814592233 | 0.3375253421 |
| 16 | 9.550497828 | 0.2807842639 | 0.3404691784 |
| 17 | 9.539400579 | 0.279815587 | 0.3431109371 |
| 18 | 9.528559648 | 0.2786397528 | 0.3455374054 |
| 19 | 9.517917168 | 0.2773191499 | 0.3478111483 |
| 20 | 9.507431359 | 0.2758986329 | 0.3499771531 |
| 21 | 9.497072069 | 0.2744103882 | 0.3520677366 |
| 22 | 9.486817529 | 0.272877477 | 0.3541060349 |
| 23 | 9.476652001 | 0.2713164005 | 0.3561086342 |
| 24 | 9.466564077 | 0.2697389512 | 0.3580873957 |
| 25 | 9.456545455 | 0.268153545 | 0.3600507967 |
| 26 | 9.446590065 | 0.2665661783 | 0.3620048898 |
| 27 | 9.436693431 | 0.2649811152 | 0.363953991 |
| 28 | 9.426852225 | 0.2634013793 | 0.3659011732 |
| 29 | 9.417063941 | 0.2618291068 | 0.3678486192 |
| 30 | 9.407326659 | 0.2602657988 | 0.3697978754 |

Fig. 12 APL PRINTOUT OF CALCULATED $NO_2$, NO, AND $O_3$ CONCENTRATIONS





Science Center
Rockwell International

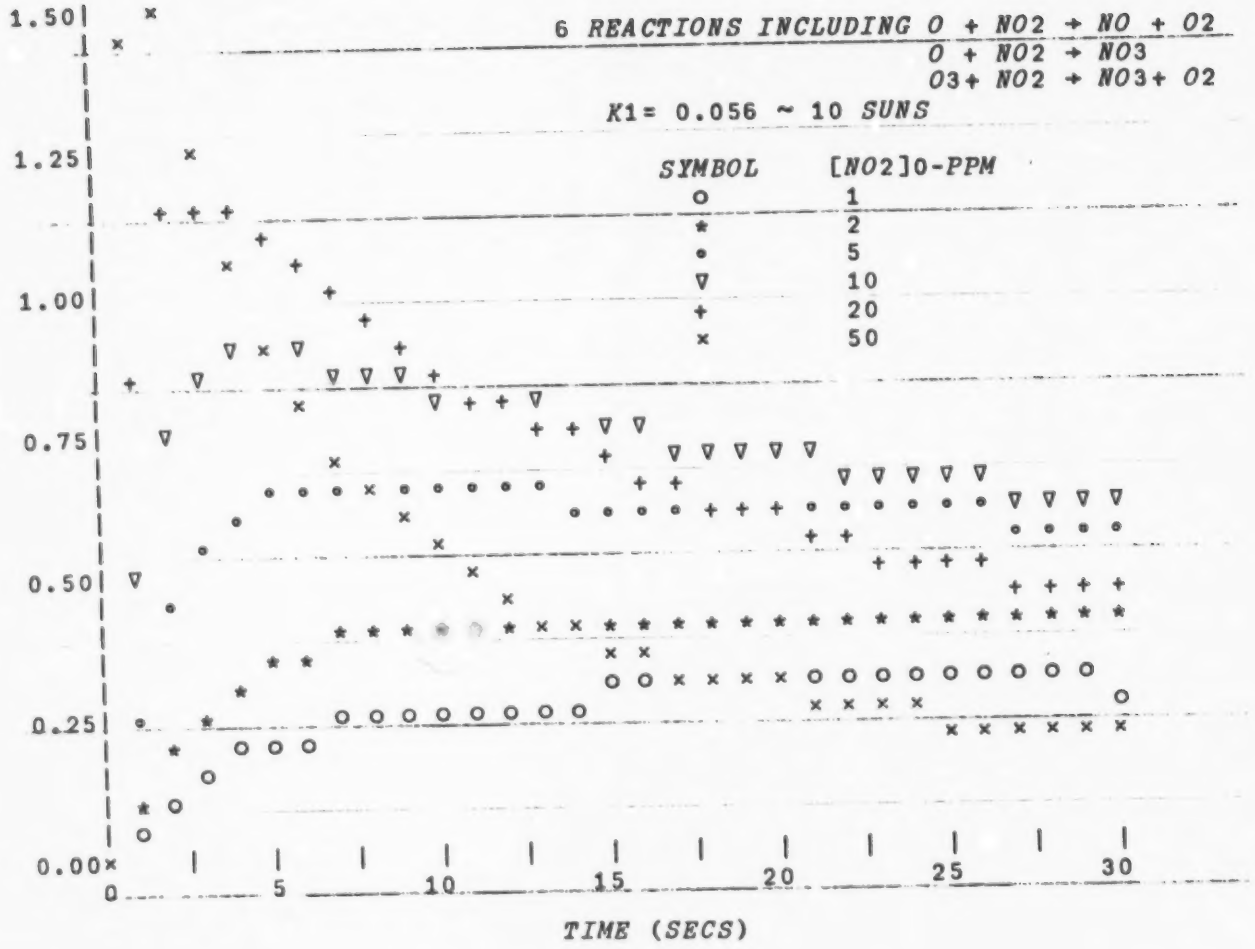


Fig. 13 AN APL PLOT OF RESULTS OF SEVERAL SETS OF CALCULATIONS OF $O_3$ CONCENTRATION

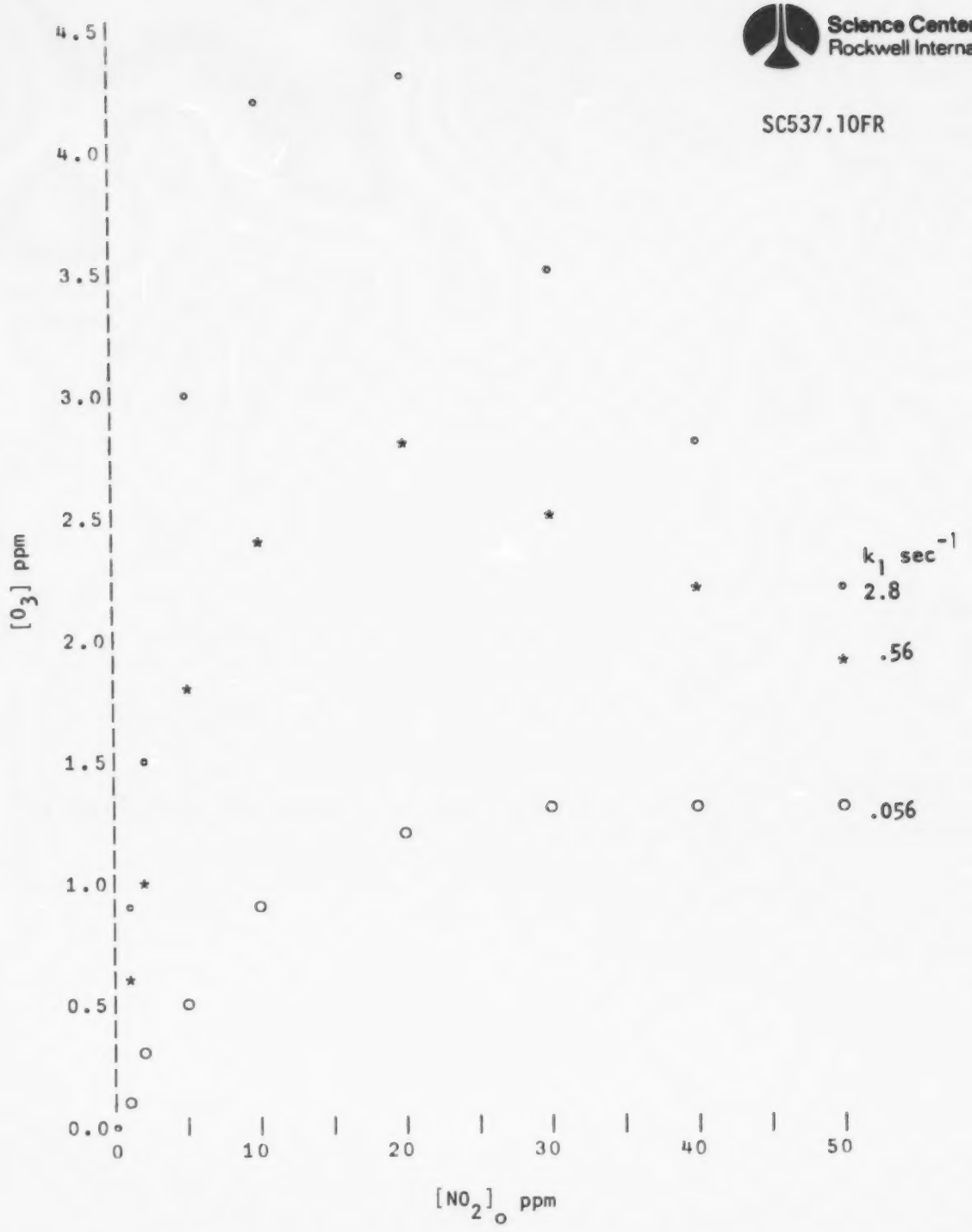


Fig. 14 - The calculated saturation of ozone production with initial $NO_2$ concentration.

Figure 15 THE INPUT SET OF REACTIONF FOR A RUN OF THE SCIENCE CENTER GENERALIZED KINETICS PROGRAM.

```
KINETICS PROGRAM

   REACTIONS USED ARE
NO2→NO+O/.008
O→O3/K=6.99E04          USE THIS CARD ONLY WHEN NOT COMPUTING O2
O3+NO→NO2/K=.383
O+NO→NO2/K=53
O+NO2→NO/K=135E00       USE THIS CARD ONLY WHEN NOT COMPUTING O2
O+NO2→NO3/36.7
NO3+NO2→N2O5/K=113
N2O5→NO2+NO3/K=.25
O3+NO2→NO3/K=.0013E00   USE THIS CARD ONLY WHEN NOT COMPUTING O2
NO3+NO→NO2+NO2/K=183
```

printout. Figure 16 shows actual computer printout of the solution to the system shown in Figure 15. In addition Calcomp plots can be prepared from the results. This program promises to be very useful in analyzing the output data from the flow reactor.

CONCENTRATIONS AS A FUNCTION OF TIME -- ALL 6 REACTANTS -IN PPM

| TIME(SECS) | NO2 | NO | NO3 | N2O5 | O | O3 | NS |
|---|---|---|---|---|---|---|---|
| 0. | .25000E-02 | .75000E-02 | 0. | 0. | 0. | 0. | |
| 1.000 | .24801E-02 | .75199E-02 | .32800E-10 | .40419E-11 | .28384E-09 | .19891E-04 | 96 |
| 2.000 | .24604E-02 | .75396E-02 | .70755E-10 | .16081E-10 | .28159E-09 | .39567E-04 | 4 |
| 3.000 | .24410E-02 | .75590E-02 | .10970E-09 | .34812E-10 | .27936E-09 | .59029E-04 | 3 |
| 4.000 | .24217E-02 | .75783E-02 | .14869E-09 | .58705E-10 | .27716E-09 | .78281E-04 | 2 |
| 5.000 | .24027E-02 | .75973E-02 | .18737E-09 | .86434E-10 | .27498E-09 | .97322E-04 | 2 |
| 6.000 | .23838E-02 | .76162E-02 | .22558E-09 | .11691E-09 | .27283E-09 | .11616E-03 | 1 |
| 7.000 | .23652E-02 | .76348E-02 | .26316E-09 | .14924E-09 | .27069E-09 | .13479E-03 | 1 |
| 8.000 | .23468E-02 | .76532E-02 | .30003E-09 | .18274E-09 | .26858E-09 | .15321E-03 | 1 |
| 9.000 | .23286E-02 | .76714E-02 | .33610E-09 | .21682E-09 | .26650E-09 | .17144E-03 | 1 |
| 10.00 | .23105E-02 | .76895E-02 | .37133E-09 | .25106E-09 | .26444E-09 | .18946E-03 | 1 |
| 11.00 | .22927E-02 | .77073E-02 | .40567E-09 | .28506E-09 | .26240E-09 | .20729E-03 | 1 |
| 12.00 | .22751E-02 | .77249E-02 | .43911E-09 | .31863E-09 | .26038E-09 | .22492E-03 | 1 |
| 13.00 | .22576E-02 | .77424E-02 | .47162E-09 | .35148E-09 | .25838E-09 | .24236E-03 | 1 |
| 14.00 | .22404E-02 | .77596E-02 | .50320E-09 | .38347E-09 | .25641E-09 | .25960E-03 | 1 |
| 15.00 | .22233E-02 | .77767E-02 | .53384E-09 | .41449E-09 | .25446E-09 | .27666E-03 | 1 |
| 16.00 | .22065E-02 | .77935E-02 | .56355E-09 | .44444E-09 | .25253E-09 | .29353E-03 | 1 |
| 17.00 | .21898E-02 | .78102E-02 | .59235E-09 | .47327E-09 | .25062E-09 | .31021E-03 | 1 |
| 18.00 | .21733E-02 | .78267E-02 | .62023E-09 | .50094E-09 | .24873E-09 | .32671E-03 | 1 |
| 19.00 | .21570E-02 | .78430E-02 | .64723E-09 | .52743E-09 | .24686E-09 | .34302E-03 | 1 |
| 20.00 | .21408E-02 | .78592E-02 | .67334E-09 | .55273E-09 | .24501E-09 | .35915E-03 | 1 |
| 21.00 | .21249E-02 | .78751E-02 | .69860E-09 | .57685E-09 | .24319E-09 | .37511E-03 | 1 |
| 22.00 | .21091E-02 | .78909E-02 | .72302E-09 | .59980E-09 | .24138E-09 | .39089E-03 | 1 |
| 23.00 | .20935E-02 | .79065E-02 | .74662E-09 | .62159E-09 | .23960E-09 | .40649E-03 | 1 |
| 24.00 | .20781E-02 | .79219E-02 | .76942E-09 | .64226E-09 | .23783E-09 | .42192E-03 | 1 |
| 25.00 | .20628E-02 | .79372E-02 | .79144E-09 | .66182E-09 | .23608E-09 | .43718E-03 | 1 |
| 26.00 | .20477E-02 | .79523E-02 | .81270E-09 | .68032E-09 | .23436E-09 | .45226E-03 | 1 |
| 27.00 | .20328E-02 | .79672E-02 | .83323E-09 | .69778E-09 | .23265E-09 | .46718E-03 | 1 |
| 28.00 | .20181E-02 | .79819E-02 | .85304E-09 | .71424E-09 | .23096E-09 | .48194E-03 | 1 |
| 29.00 | .20035E-02 | .79965E-02 | .87215E-09 | .72973E-09 | .22929E-09 | .49652E-03 | 1 |
| 30.00 | .19890E-02 | .80110E-02 | .89059E-09 | .74428E-09 | .22764E-09 | .51095E-03 | 1 |
| 31.00 | .19748E-02 | .80252E-02 | .90838E-09 | .75794E-09 | .22601E-09 | .52521E-03 | 1 |
| 32.00 | .19607E-02 | .80393E-02 | .92556E-09 | .77073E-09 | .22440E-09 | .53931E-03 | 1 |
| 33.00 | .19467E-02 | .80533E-02 | .94216E-09 | .78269E-09 | .22280E-09 | .55326E-03 | 1 |
| 34.00 | .19329E-02 | .80671E-02 | .95794E-09 | .79385E-09 | .22122E-09 | .56705E-03 | 1 |
| 35.00 | .19193E-02 | .80807E-02 | .97326E-09 | .80425E-09 | .21966E-09 | .58068E-03 | 1 |

Figure 16 PRINTOUT OF A COMPLETE NUMERICAL SOLUTION OF SYSTEM SHOWN IN FIG. 15.

## Appendix B. Aerosol Forming Reactions with Ozone and Olefins in a Flow Reactor

One of the problems that developed early in this feasibility study involved questions of time scaling for aerosol formation in reactive gases. Furthermore, samples of aerosols analogous to those expected to be generated by photochemical reactions were required to test and validate sampling methods and schemes for chemical analysis. In a complementary program sponsored by the Science Center, work was started to investigate airborne particle formation resulting from chemical reactions and a series of olefin vapors. Such reactions may be important in photochemical smog. After determining the feasibility of forming aerosols by such reactions, the formation rate was investigated, and samples of the condensed material were used to develop chemical analysis techniques for the APRAC sponsored program.

### B.1 Experimental Methods

The aerosol forming reactions of olefins and ozone were investigated in a steady flow system made of a pyrex pipe 3 meters long and 5.1 cm in diameter. Ozone was generated in a stream of oxygen by ultraviolet radiation; this flow was mixed in the flow reactor with a dry nitrogen stream (< 10 ppm $H_2O$ vapor) containing olefins at the ppm concentration level. Gas flows into the reactor were measured using rotameters.

The olefins studied included 1-butene, 1-hexene, and 1-octene; however, the one of principal interest was 1-butene.

The ozone concentration was measured at the exit of the reactor with and without the presence of olefin using a KI titration method or a REM chemiluminescent ozone monitor, calibrated with a KI titration procedure.

Reaction times, based on the mean gas flow through the reactor were set to range between 20 sec and 1 minute. Flow was kept sufficiently low to retain a laminar flow.

Sampling for aerosol was conducted by a glass tube centered in the pipe axis. The sampling tube could be pushed into the pipe up to 1½ meters to vary the reaction time. Shorter pipes also were used to vary the reaction time.

Qualitative tests for the sensitivity to water vapor or to aldehyde vapors were performed by adding such constituents with the nitrogen stream at the reactor entrance. Tests have been made with water vapor, acetaldehyde, and butyaldehyde.

Aerosol production was measured by several means. The physical properties were observed using the following instrumentation:

a. Total number concentration - GE Aitken Nuclei Counter
b. Total mass concentration - glass fiber filter
c. Particle size distribution - Portable Whitby - Liu electrical mobility analyzer
d. Visible light scattering - laser beam and Royco 225 optical counter

The chemical properties were derived from examination of filter collected samples using infrared spectroscopy, gas chromatography-mass spectroscopy, iodimetry and electrochemistry. The infrared spectra were obtained using a Perkin Elmer Model 421 Infrared Spectrometer. This instrument is a double grating spectrometer with resolution of 0.3 $cm^{-1}$. Both extraction and pellet techniques were employed. The technique used for the iodide oxidation measurements was standard using sodium thiosulfate to titrate the $I_2$ produced with starch as the indicator. The polarographic measurements were made with an instrument constructed in this laboratory.[39]. For the GC-MS system a Loenco Model 15B gas chromatograph was used with an inlet system especially designed to allow the pyrolysis products to enter the gas chromatograph in a "slug." The GC carrier gas is separated from the sample material using an effusion orifice and a silver membrane enricher. The CEC 21-103C mass spectrometer used was modified to allow a scan of the accelerating voltage to be made within two seconds with repetitive scans every three seconds. This gives a sweep from mass number 26 to 150. This was done by an in-house designed and constructed scan control system which operates in conjunction with the Dempster configuration of the mass spectrometer to give a linear relation between mass number and time. A Honeywell Visicorder was used to record mass spectral patterns at the appropriate times. In addition, a DEC PDP-11 computer has been interfaced with the MS output to allow peak height

vs. time to be obtained and stored on a disk memory. Provision has been made to reduce and store 500 peaks per scan with a total number of scans per analysis of 20,000. The data are reduced by FORTRAN programs, which give various types of information such as normalized total ionization vs. scan number.

B.2 Experimental Results & Discussion

The study showed that aerosol can be generated in a dry nitrogen steam in a mixture containing ppm (to tens ppm) level ozone and ppm (to tens ppm) level olefin beginning with 1-butene over an average residence time of less than a minute. The production of Aitken nuclei in the reactor for different olefins is shown in Fig. 17. Here there is evidence that aerosol production rate is enhanced, for a given residence time, using olefins of carbon number higher than four. The increase in nuclei production rate is very sharp with increasing olefin concentration suggesting an effective "threshold" for nucleation of condensed phase in the reactor. This indicates that the rate of production of new nuclei is highly non-linear and can be expected to be very slow or negligible, for olefins of molecular weight lower than 50-80, at the ppb level in a stream containing ppm level or lower ozone.

At concentrations of reactants higher than a few ppm, particles of size sufficient to scatter light were easily seen using a laser beam flashed through the pipe cross-section.

A limited number of tests of the 1-butene-ozone system were conducted using a new portable Whitby-Liu electrical mobility analyzer as the aerosol detector. The aerosol volume distribution as well as the total surface to volume ratio can be derived from measurements using this device. The change in (volume) size distribution with increasing 1-butene concentration is shown in Fig. 18. This set of curves indicates that the early stages of nucleation and growth by condensation of material generates an aerosol with a weak increase in mean particle size from ~ 0.07 μm to ~ 1.0 μm, but with material accumulating primarily in the particle sizes below 0.1 μm diameter.

Volume distributions corresponding to increases in residence time are shown in Fig. 19. These results indicate the changes in the aerosol formed

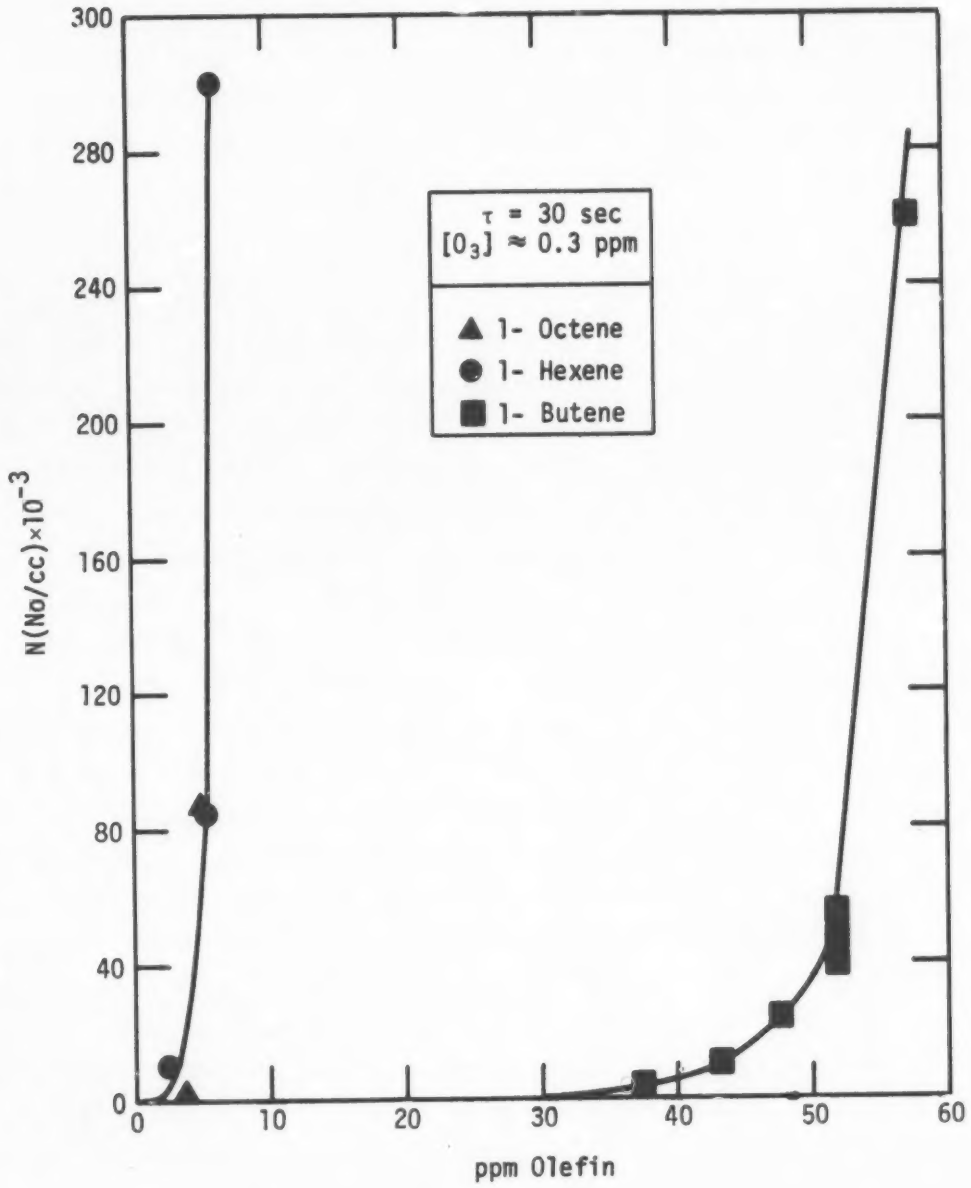


Figure 17 PRODUCTION OF AEROSOLS FROM OLEFINS, AS MEASURED BY AITKEN NUCLEI CONCENTRATION.

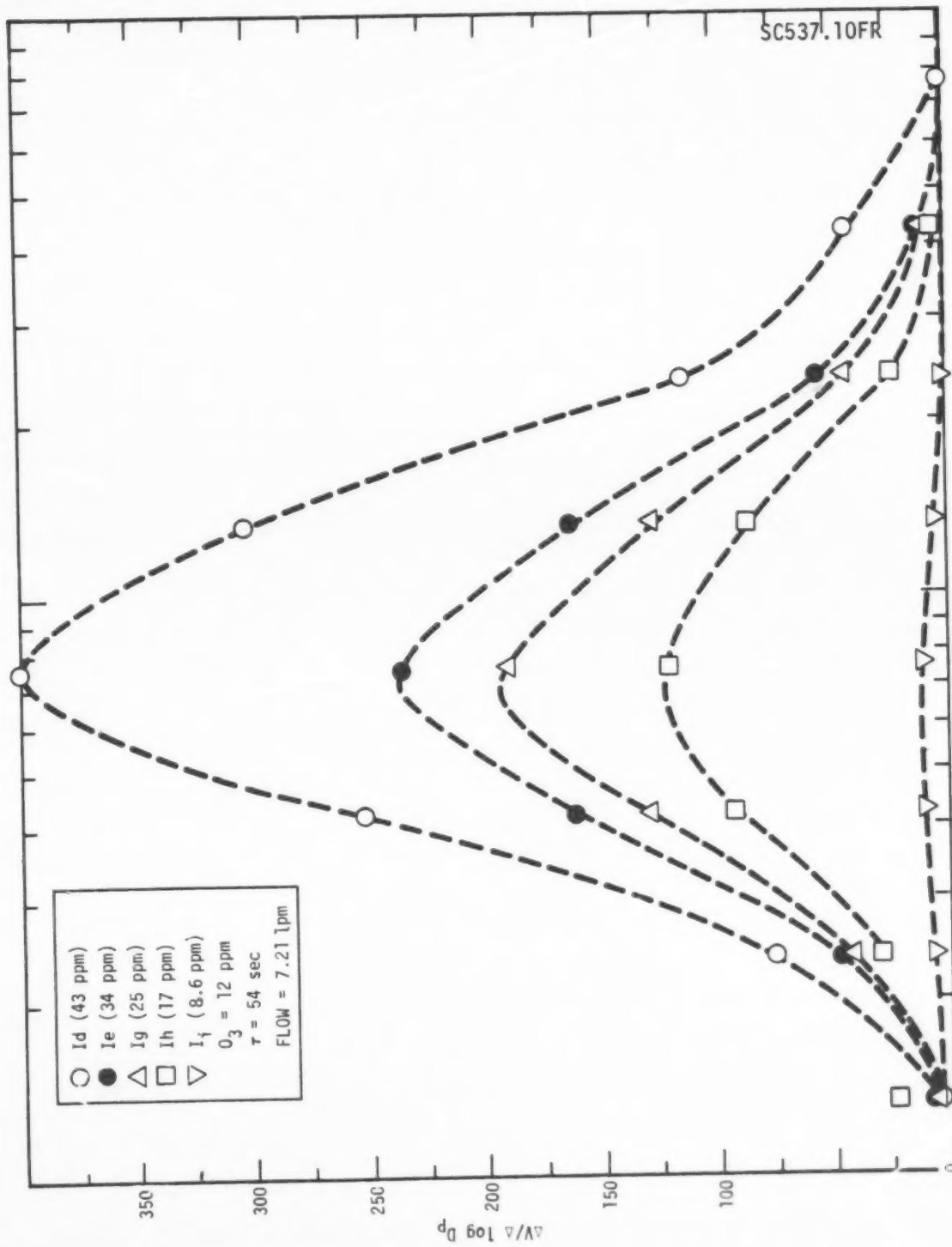


Figure 18 VOLUMETRIC SIZE DISTRIBUTION AS A FUNCTION OF 1-BUTENE CONCENTRATION IN THE FLOW REACTOR.

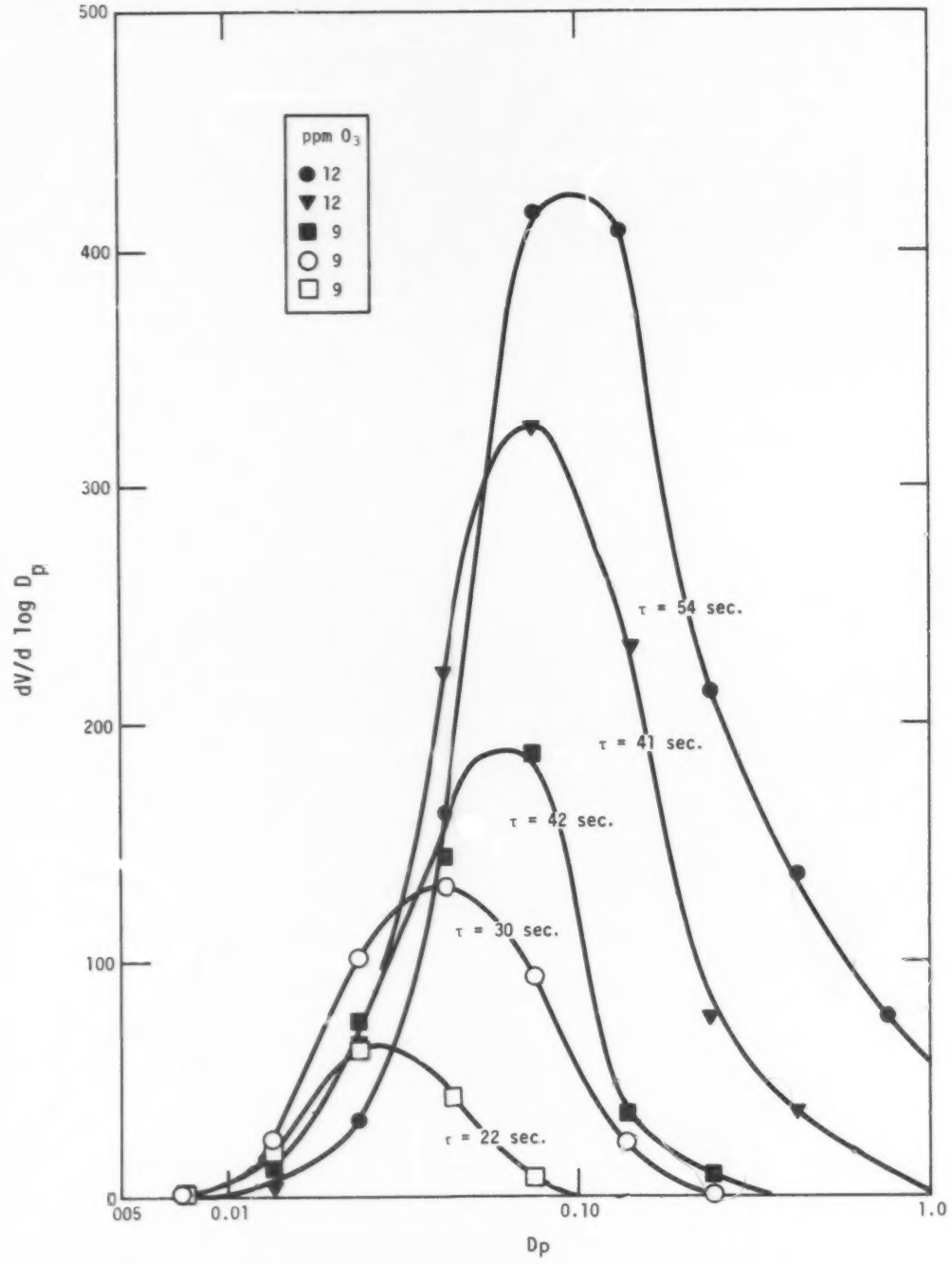


Figure 19 EVOLUTION OF AEROSOL SIZE DISTRIBUTION GENERATED FROM THE REACTION OF OZONE AND 1-BUTENE.

at constant (initial or upstream) reactant concentrations with time. There is an increase in mean particle size with increasing time indicating qualitatively the complementary effects of nucleation, growth by condensation and coagulation of particles. That is, there is a decrease in the volume of smallest particles accompanied by a generation of larger particles and a systematic shift in mean particle size to larger sizes.

The changes in number concentration (<N>) and mean volume concentration (<v>) with changes in 1-butene and ozone are shown in Figs. 20 and 21. In both cases, there is a sharp initial increase in airborne material showing a "threshold" analogous to the increase in nuclei concentration in Fig. 10. At higher reactant concentration the nuclei production rate tapers off, but the surface and volume continue to increase. The data for variation in volume production rate with reactant concentration are semi-quantitative in nature but indicate that the generation of condensed phase is non-linear in both olefin and ozone.

It is interesting to compare the collection of mass on a filter with the measurements of the electrical mobility analyzer. Such a comparison is shown in Fig. 22 for the volume concentration estimated from the analyzer. Assuming that the condensed material has a constant density, there is a major difference between the filter collected mass and that projected from the electrical mobility analyzer. The filter collects considerably more material than expected and the accumulated material appears to increase linearly with butene concentration rather than non-linearly. This result points to the critical problem of sampling for aerosols in a chemically reactive gas mixture. In this case, the filter substrate may be acting as a reactive surface for production of condensed material. On the other hand the filter is larger in diameter, nearly as large as the pipe, and will be accumulating significant amounts of aerosol from slower moving regions of gas (longer residence times) than the sampling tube used for the analyzer. The analyzer tubing may contribute to some loss of aerosol, too, prior to reaching the instrument. Further work is needed on this problem before such data can be interpreted intelligently.

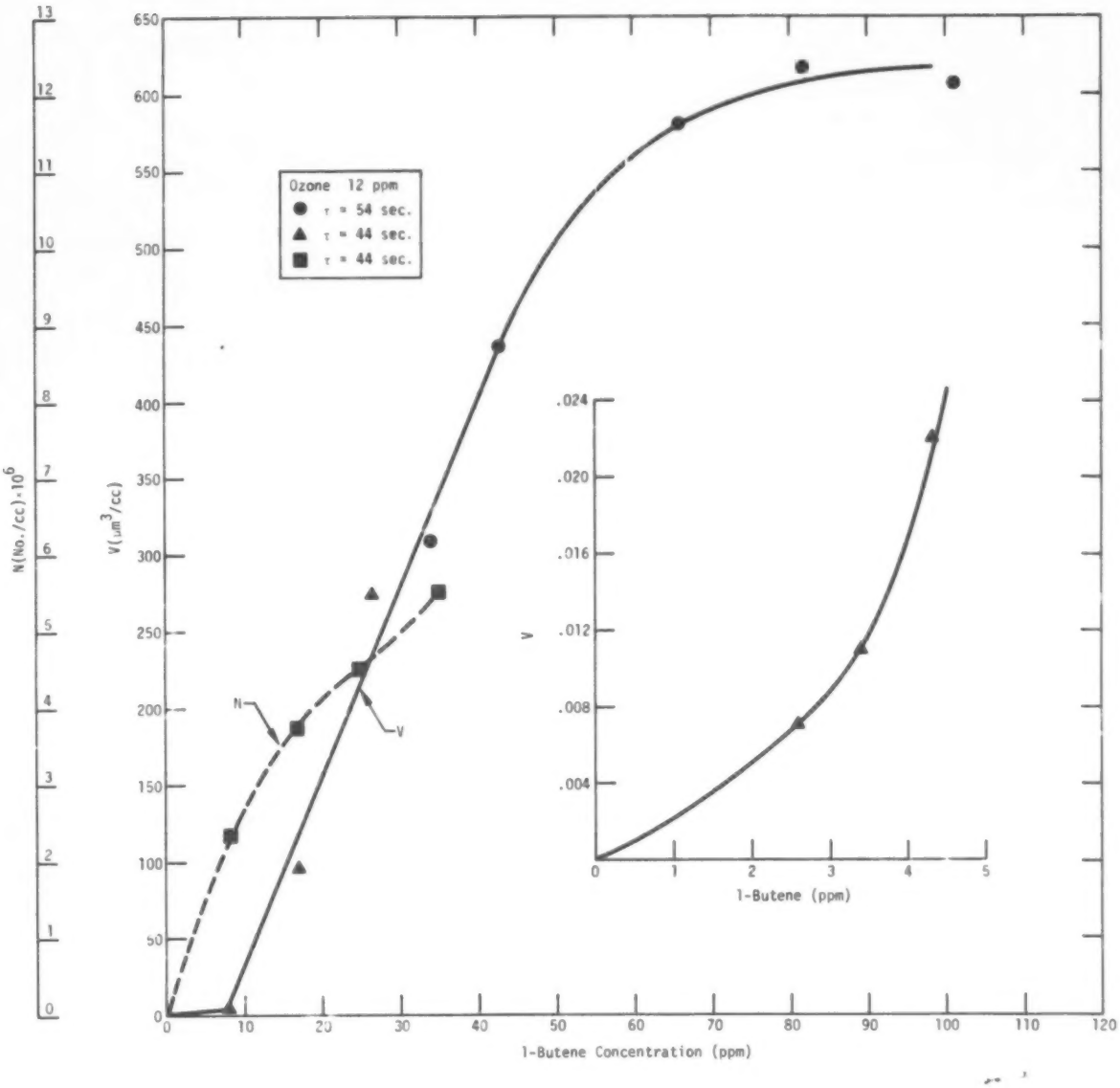


FIGURE 20 VARIATION WITH 1-BUTENE OF TOTAL NUMBER AND VOLUME CONCENTRATION OF AEROSOLS PRODUCED FROM A REACTION OF OZONE AND 1-BUTENE.

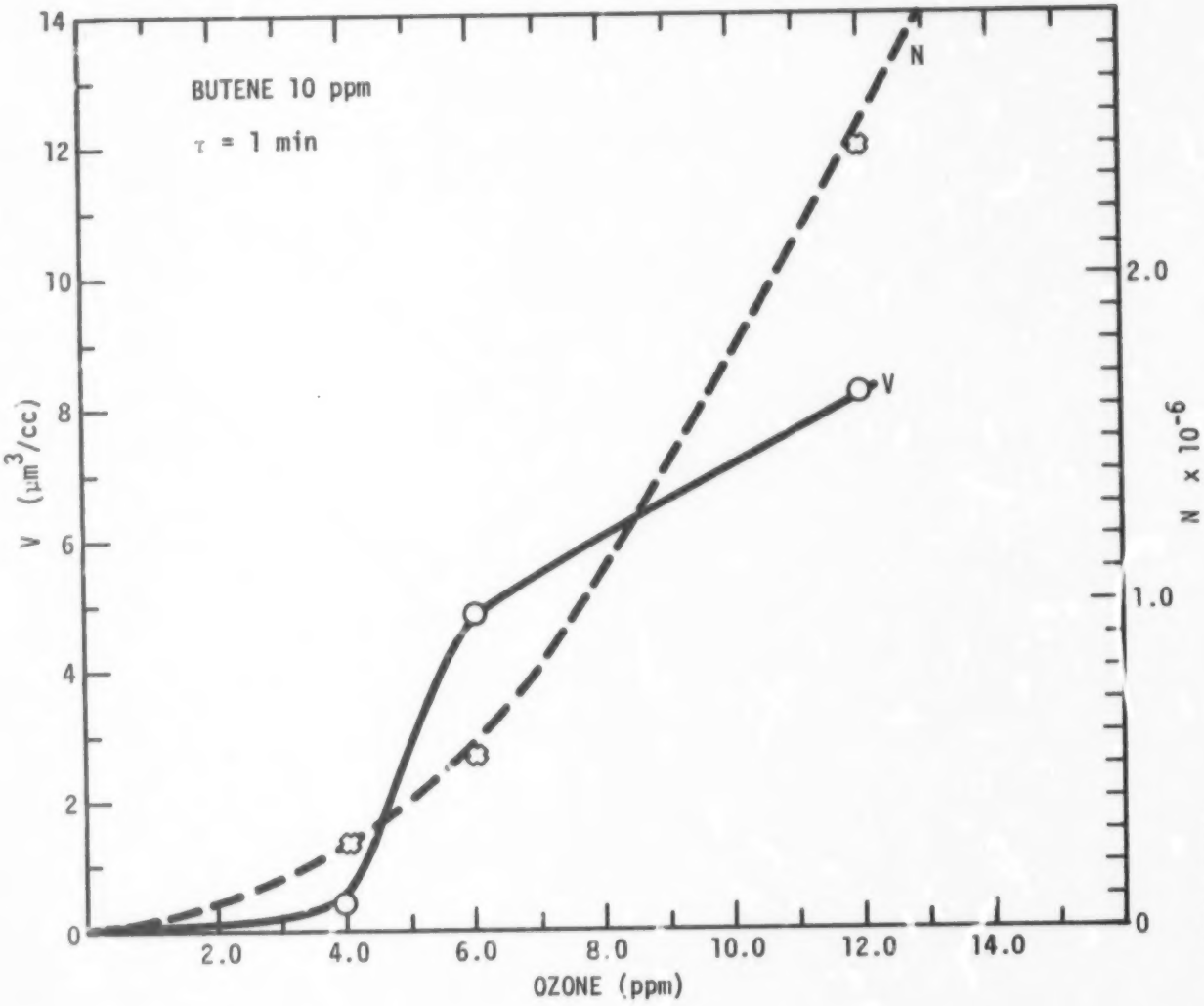


Figure 21 CHANGE IN NUMBER AND VOLUME CONCENTRATION WITH INCREASE IN OZONE CONCENTRATION.



SC537.10FR
Science Center
Rockwell International

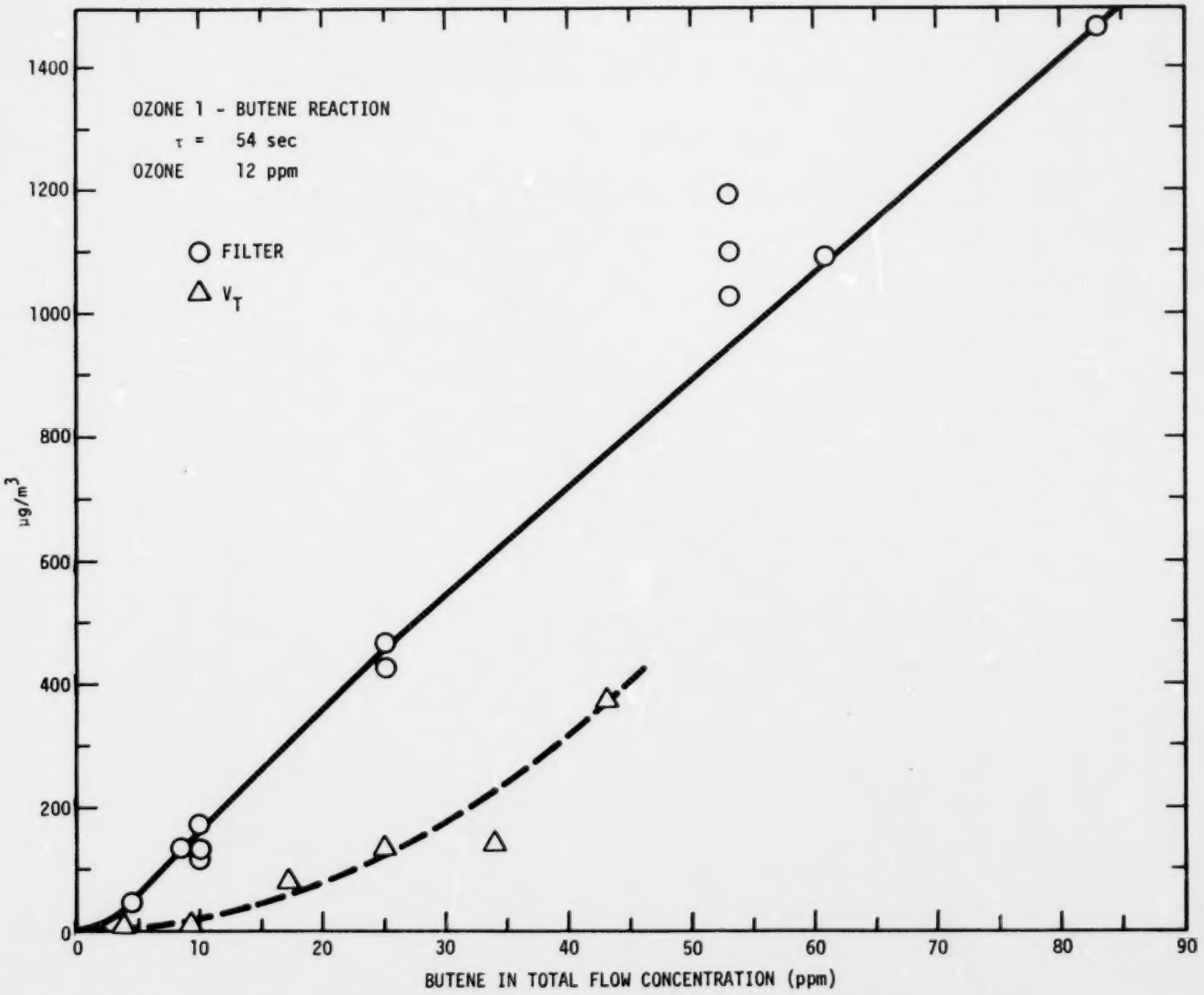


Figure 22 COMPARISON BETWEEN MASS CONCENTRATION FROM GLASS FIBER FILTER COLLECTION AND ESTIMATED FROM THE WHITBY ELECTRICAL MOBILITY ANALYZER ASSUMING A DENSITY OF UNITY.

## B.3 Chemical Analysis of Ozone-Olefin Aerosol

The chemical analysis of the filter collected material from the ozone-1-butene reactions revealed that its composition was organic, with highly oxygenated constituents.

Freshly prepared aerosol will readily oxidize iodide. If the material stands for longer than a week, it no longer will react. It has been found that an oxidation equivalent of approximately 0.01 meq/mg is obtained on a fresh sample. This apparent reactivity would suggest that the sample contains either a peroxide or an ozonide. Using the method of Mair and Graupner,[40] it has been shown that the "Method 1" or easily reduced peroxide is responsible for iodide oxidation. The positive half wave potential of the reduction wave of the material in a fresh aerosol sample also suggests that the material falls into the class of easily reduced peroxides[41] [e.g. diacyl peroxides, hydro peroxides, etc.].

Examination of infrared spectra and gas chromatography-mass spectroscopy combination data also suggests a possible peroxide or ozonide but the identification is still not clarified. Fig. 23 shows the infrared spectrum of an aerosol by transfer of the material to an Irtran window. The general similarity of this IR spectrum to those obtained from ambient aerosol and smog chambers is interesting.[30] Table 8 shows two GC-MS analyses of filter collected aerosol samples. Table 9 shows a comparison of mass spectral data obtained from one gas chromatograph peak with the known compound and with the reference spectral pattern. The differences between the calibration pattern and the ASTM pattern is caused by different mass discrimination resulting from the use of different mass spectrometers and detectors.

One of the problems with identification of the aerosol composition is associated with its potential complexity. In order to get specific identification of the components of the material, it appears to be necessary to attempt a separation of the product mixture. The use of thin layer chromatography and paper chromatography have been used on peroxide mixtures[41] and these techniques are currently being tried.

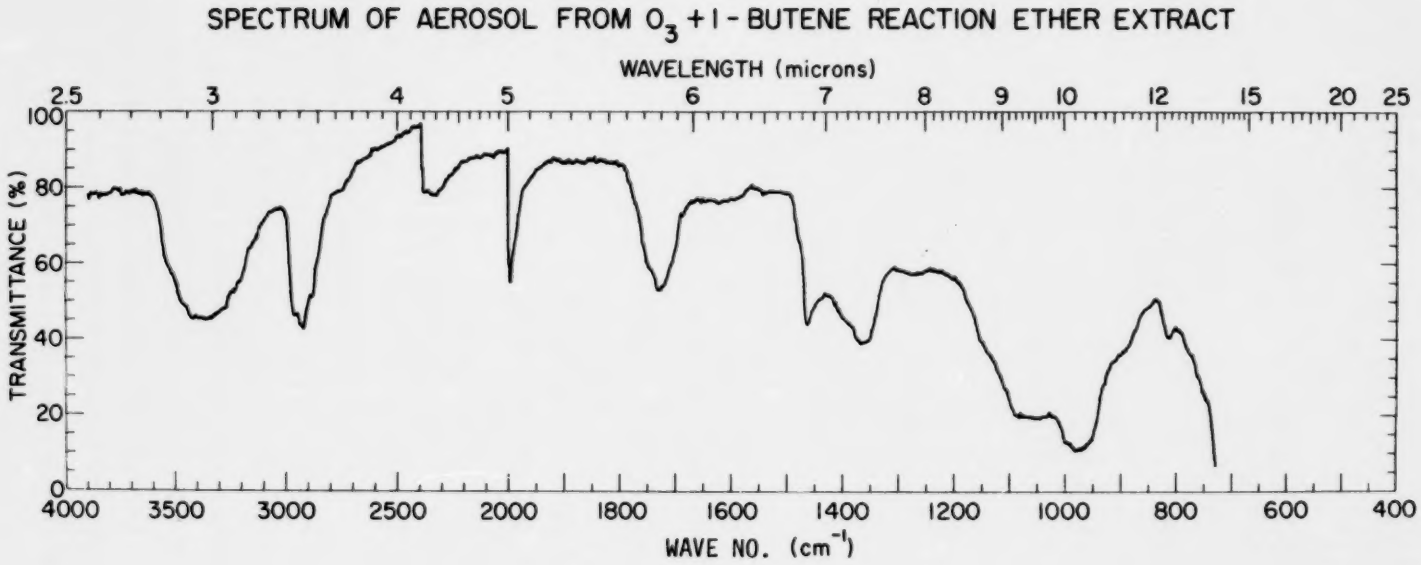


FIGURE 23 INFRARED SPECTRUM OF THE ETHER EXTRACT OF FILTER COLLECTED AEROSOL PRODUCED FROM THE REACTION OF OZONE AND 1-BUTENE.

Table 8

IDENTIFICATION BY GC-MS OF APPARENT PYROLYSIS PRODUCTS OF AEROSOLS OBTAINED FROM OZONE 1-BUTENE GAS PHASE REACTION

| GC Peak Number | Run 1 | Run 2 | Identity |
|---|---|---|---|
| 1 | 9.8*% | 11.7*% | Carbon Dioxide |
| 2 | 0.03 | | |
| 3 | 0.09 | | |
| 4 | 0.6 | 0.5 | Ethane |
| 5 | 19.7* | 34.6* | Water |
| 6 | 10.1 | 6.7 | Formaldehyde |
| 7 | 0.4 | 0.6 | Methanol |
| 8 | 3.5 | 5.2 | Acetaldehyde |
| 9 | 44.5 | 29.2 | Formic Acid |
| 10 | 19.1 | 18.5 | Propionaldehyde |
| 11 | 1.8 | 1.7 | Acetic Acid |
| 12 | 0.3 | | |
| 13 | 14.6 | 12.7 | Propionic Acid |
| 14 | 0.06 | | |
| 15 | 2.2 | 2.2 | |
| 16 | 0.3 | | |
| 17 | 0.1 | | |
| 18 | 1.8 | 1.0 | |
| 19 | 0.4 | | |
| 20 | 0.3 | | |
| % Identified | 94.6 | 96.8 | |

*% of total sample but excluded from other percentage calculations. % refers to peak area percentage assuming equal thermal conductivity detector sensitivity. Run 1: 6 mg total aerosol. Run 2: 12 mg total aerosol.

Table 9

COMPARISON OF MASS SPECTRAL PATTERNS FOR PROPIONIC ACID OBTAINED FROM AEROSOL DECOMPOSITION AND FROM CALIBRATION SAMPLE AND REFERENCE SPECTRUM

| M/e | Peak 10 From Aerosol | Calibration Known (Propionic Acid) | ASTM #302 |
|---|---|---|---|
| 26 | 21 | 24 | 21.1 |
| 27 | 62 | 60 | 61.7 |
| 28 | 100 | 100 | 100 |
| 29 | 86 | 83 | 83.6 |
| 30 | 10 | 11 | 14.1 |
| 45 | 31 | 33 | 55.7 |
| 55 | 7.5 | 9 | 16.8 |
| 56 | 6.2 | 6 | 16.4 |
| 57 | 15 | 18 | 30.1 |
| 73 | 24 | 34 | 48.4 |
| 74 | 37 | 53 | 75.8 |

## REFERENCES

1. Tyndall, J., Phil. Mag. S4 37, 384 (1969).

2. Robinson, E. and Robbins, R. C., "Gaseous Atmospheric Pollutants from Urban and Natural Sources" in Global Effects of Environmental Pollution, S. Fred Singer, Editor, Springer-Verlag, New York, 1970.

3. Leighton, P. A., "Photochemistry of Air Pollution," Academic Press, N.Y., 1961.

4. Wilson, W. E., Jr. and Levy, A., JAPCA 20, 385 (1970); Wilson, W.E., Jr., Merryman, E.L., Levy, A., and Taliaferro, H. R., JAPCA 21, 128 (1971).

5. Stevenson, H. J. R., Sanderson, D. E., and Altshuller, A. P., Int. J. Air Water Poll. 9, 367 (1965).

6. Groblicki, P. J. and Nebel, G. J., "The Photochemical Formation of Aerosols in Urban Atmospheres," in Chemical Reactions in Urban Atmospheres, C. A. Tuesday, Editor, Elsevier, N.Y., 1971.

7. Cox, R. A. and Penkett, S. A., "Aerosol Formation from Sulfur Dioxide in the Presence of Ozone and Olefinic Hydrocarbons," J. Chem. Soc., Faraday Trans. 1 68, 1735 (1972).

8. Bricard, J., Billard, F., and Madelaine, G., J. Geophys. Res. 73, 4487 (1968).

9. Goetz, A. and Pueschel, R. F., JAPCA 15, 90 (1965).

10. National Air Surveillance Network (NASN), "Air Quality Data from the National Air Surveillance Networks and Contributing State and Local Networks," 1966 Edition, U.S. Dept. HEW, Durham, N.C., 1968.

11. Hidy, G. M. and Friedlander, S. K., "The Nature of the Los Angeles Aerosol," in the Proc. 2nd IUAPPA Clean Air Congr., Editor, Englund, H. M. and Beery, W. T., Academic Press, N.Y., 1971.

12. Miller, M. S., Friedlander, S. K., and Hidy, G. M., "A Chemical Element Balance for the Pasadena Aerosol," in reference (15).

13. D. S. Covert, R. J. Charlson, N. C. Alquist, J. Applied Meteorology 11-968 (1972).

14. Interim Report, California Aerosol Characterization Study, Science Center, Rockwell International, Thousand Oaks, CA, in preparation, April 1973.

15. Hidy, G. M., Editor, Aerosols and Atmospheric Chemistry, Academic Press, N.Y., 1972.

16. Husar, R. B., Whitby, K. T., and Liu, B. Y. H., "Physical Mechanisms Governing the Dynamics of Los Angeles Smog Aerosol," in reference (15).

17. Hidy, G. M., Mueller, P. K., Tokiwa, Y, and Twiss, S., "Aerometric Factors Affecting the Evolution of the Pasadena Aerosol," in reference (15).

18. Altshuller, A. P. and Bufalini, J. J., Env. Sci. Tech. 5, 39 (1971).

19. Bufalini, M., Env. Sci. Tech. 5, 685 (1971).

20. Westerberg, K., Cohen, N., and Wilson, K. W., Science 171, 1013 (1971).

21. Gay, B. W. and Bufalini, J. J., Env. Sci. Tech. 5, 442 (1971).

22. Friedlander, S. K. and Seinfeld, J. H., Environ. Sci. Technol. 3, 1175 (1969); Hecht, T. A. and Seinfeld, J. H., ibid., 6 47 (1972).

23. Demerjian, K. L., Kerr, J. A., and Calvert, J. G., "The Mechanism of Photochemical Smog Formation," Chemistry Department, Ohio State University, 1972.

24. Niki, H., Daby, E. E., and Weinstock, B., "Mechanisms of Smog Reactions," in R. E. Gould, Editor, "Photochemical Smog and Ozone Reactions," Advances in Chemistry, Series 113, Am. Chem. Society, Washington, D.C. (1972).

25. Haagen-Smit, A. J., Ind. Eng. Chem. 44, 1342 (1952).

26. Doyle, G. J. and Renzetti, N. A., JAPCA 8, 23 (1958; Renzetti, N. A. and Doyle, G. J., ibid. 8, 293 (1959); Renzetti, N. A. and Doyle, G. J., Int. J. Air Poll. 2, 237 (1960); Doyle, G. J. and Jones, J. L., JAPCA 13, 365 (19 3); Endow, N., Doyle, G. J., and Jones, J. L., ibid. 13, 141 (1963).

27. Prager, M. J., Stephens, E. R., and Scott, W. E., Ind. Eng. Chem. 52, 521 (1960).

28. Goetz, A. and Kallai, T., JAPCA 12, 437 (1962); Goetz, A. and Kallai, T. J. Am. Ind. Hyg. Assoc. 24, 453 (1963); Goetz, A. and Pueschel, R. F., Atm. Env. 1, 287 (1967).

29. Harkins, J. and Nicksic, S. W., JAPCA 15, 218 (1965).

30. Wilson, W. E., Jr., Schwartz, W. E., and Kinzer, G. W., "Haze Formation -- Its Nature and Origin," Battelle Columbus Laboratories, Jan. 28, 1972.

31. Generalization of equation (16) from reference (32).

32. Ferguson, E. E., Fehsenfeld, F. C., and Schmeltekopf, A. L., "Flowing Afterglow Measurements of Ion-Neutral Reactions," in Advances in Atomic and Molecular Physics, Editor, Bates, D. R., Academic Press, N.Y., 1969.

33. Cher, M. and Hollingsworth, C. S., "Chemiluminescent Reactions of Excited Helium with Nitrogen and Oxygen," Advances in Chemistry Series 80, 118 (1969).

34. Crank, J., "The Mathematics of Diffusion," Oxford University Press, N.Y., 1957, pages 66-67.

35. Dushman, S., Scientific Foundations of Vacuum Technique, 2nd ed., John Wiley and Sons, Inc., N.Y., 1962.

36. National Research Council, International Critical Tables 5, 62 (1929).

37. Fuchs, N. A., The Mechanics of Aerosols, Pergamon Press, N.Y., 1964.

38. Chapter 4, Section 26 of reference (37).

39. Parry, E. P. and Osteryoung, R. A., Anal. Chem. 36, 1366 (1964).

40. Mair, R. D. and Grapuner, A. S., Anal. Chem. 36, 194 (1964).

41. Mair, R. D. and Hall, R. T. in Organic Peroxides, edited by Swern, D., Vol. II, John Wiley and Sons, New York, 1971, see Chapter VI.

42. Ottenstein, D. M. and Bartley, D. A., "Improved Gas Chromatography Separation of Free Acids $C_2$-$C_5$ in Dilute Solution," Anal. Chem. 43, 952, 1971.

43. Cvetanovic, R. J., "Addition of Atoms to Olefins in the Gas Phase" in Advances in Photochemistry, Vol. 1, Editors, Noyes, W. A., Jr., Hammond, G. S., and Pitts, J. N., Jr., Interscience Publishers, N.Y., 1963.

Sato, S. and Cvetanovic, R. J., "The Effect of Molecular Oxygen on the Reaction of Oxygen Atoms with cis-2-Pentene," Canadian J. Chem. 37, 953, 1959.

44. Altshuller, A. P., Kopczynski, S. L., Lonneman, W. A., Becker, T. L., and Stater, R., "Chemical Aspects of the Photooxidation of the P pylene-Nitrogen Oxide System," Env. Sci. Tech. 1, 899, 1967.

45. Ellis, C. F., "Sunlight Photooxidation of Isobutylene and Butene-1 with $NO_2$ in Low-and High-Oxygen Concentrations," Atmospheric Environment 5, 83, 1971.

46. Scarengelli, R. P. and Rehme, K. A., Anal. Chem. 41, 707 (1969).

47. Huntzicker, James J., California Institute of Technology, private communication.

48. Fritz, J. S. and Yamamura, S. S., Anal. Chem. 27, 144 (1955).

49. Benarce, M. and Nonet, A., Atmos. Environ. 6 (11), 45 (1972).

50. Methods of Air Sampling and Analysis published by American Public Health Assoc., 1972, p. 322.

51. West, P. W. and Lyles, G. L., Anal. Chem. Acta 23, 227 (1960).

52. Sawicki, E., Johnson, H., and Stanley, T. W., Anal. Chem. 35, 134 (1963).

53. Parry, E. P. and Osteryoung, R. A., Anal. Chem. 37, 1634 (1965); Parry, E. P., Johnston, W., and Goldner, H. J., J. Electroanal. Chem. 13, 127 (1967); Parry, E. P. and Oldham, K. B., Anal. Chem. 40, 1031 (1968).

54. Polarography by Kolthoff, I. M. and Lingane, J. J., Vol. II, 2nd ed., Interscience, New York, 1952, p. 536.

55. Lipeles, M. and Malmuth, N., "Analytical Smog Kinetics," Environ. Sci. Tech. 6, 360-365, 1972.

56. Bridgman, P. W., Dimensional Analysis, Yale University Press, New Haven, 1931.

57. Birkhoff, G., Hydrodynamics, Dover, N.Y., 1950.

58. Hidy, G. M., "On Atmospheric Simulation: A Colloquium," NCAR-TN-22 Report of National Center for Atmospheric Research, Boulder, Colorado, 1966.

59. Gear, C. W., Communications of the ACM 14, 176, 1971.

60. Whitby, K. T., Husar, R. B., Liu, B. Y. H., "The Aerosol Size Distribution of Los Angeles Smog" in reference (15).